Plant-microbe-mediated decrease of greenhouse gases under dynamic wetland hydrology

Regina B. Bledsoe[1,2], Colin G. Finlay[1,*], Ariane L. Peralta[1]

1. Department of Biology, East Carolina University, Greenville, NC 27858, USA
2. NewLeaf Symbiotics, St. Louis, MO 63132, USA

*Corresponding author: telephone: +1 307.690.1734, e-mail: finlayc21@students.ecu.edu

Regina B. Bledsoe and Colin G. Finlay are co-first authors.

Open Research statement: All code and data used in this study are in a public GitHub repository (https://github.com/PeraltaLab/WetlandMesocosm_GHG_Timberlake) with a Zenodo DOI (https://doi.org/10.5281/zenodo.15528281). Raw amplicon sequence files can be found at NCBI SRA BioProject ID PRJNA636184, and metagenome sequence files can be found at NCBI SRA BioProject ID PRJNA641216.

Key words/phrases: 16S rRNA; carbon dioxide; denitrification; greenhouse gases; hydrology; metagenomics; methane; nitrous oxide; plant cover; plant-microbe interactions; soil mesocosms; soil redox

Abstract

While wetlands represent a small fraction (~5-10%) of the world's land surface, it is estimated that one-third of wetlands have been lost due to human activities. Wetland habitat loss decreases ecosystem benefits such as improving water quality and mitigating climate change. These microbially mediated functions are dependent on redox conditions, which are altered by soil hydrology and the presence of plants. In this study, we hypothesized that redox status due to continuous flooding would support greater abundance of microbial taxa involved in methanogenesis (obligate anaerobes), but plant-mediated oxygen transport would decrease methane emissions. Using a mesocosm design, we manipulated the duration of hydrologic conditions (i.e., stable dry, stable flooding, and alternating wet/dry) and presence of plants to induce soil redox changes in wetland soils. We measured soil redox status, used targeted amplicon and shotgun metagenomic sequencing to characterize microbial communities, and measured greenhouse gas production to assess microbial function. Results showed that hydrologic history influenced microbial community composition while plant presence and hydrologic treatment altered microbial functional gene composition to a lesser degree. Plant presence decreased carbon dioxide fluxes, while differences in the community composition of functional genes related to carbohydrate metabolism, denitrification, and methanogenesis also explained variation in emissions of carbon dioxide and, to a lesser extent, methane. While previous studies do not often include plants when assessing greenhouse gas emissions, this study highlights that plant-mediated decreases in greenhouse gas emissions are important, and plant-mediated effects should be considered when estimating the carbon balance of ecosystems.

43 **Importance**

44 This study revealed that initial hydrologic conditions, compared to manipulated
45 hydrology, strongly influenced microbial community composition more than their function.
46 Specifically, results showed that hydrology is a strong environmental filter that determines
47 microbial taxonomic and functional community patterns, short-term redox changes that are most
48 distinct from historic redox conditions shift microbial communities, and plant presence can
49 stabilize redox shifts and mediate greenhouse gas production. These results underscore the
50 importance of plant presence and the duration of flooding and drying periods in influencing
51 wetland greenhouse gas production.

52

Introduction

Wetlands represent only 5-10% of terrestrial land surface (Kingsford, Basset, and Jackson 2016); however, it is estimated that we have lost at least 21% of wetlands as of 2023 (Fluet-Chouinard et al. 2023). Loss of essential functions is a consequence of the land use conversion of wetlands to urban and agricultural development. These wetland ecosystems provide valuable services, including improving water quality by decreasing nutrient and pollutant loads, and mitigating climate change by sequestering carbon. Therefore, there is an interest in conserving, restoring, and constructing wetlands for these ecosystem benefits. Examples of valuable wetland ecosystem functions include anaerobic microbial processes associated with saturated soils, which promote the complete removal of inorganic nitrogen via denitrification (NO_3 to N_2) and suppress the aerobic decomposition of organic matter. These same anoxic soil conditions can also support methane (CH_4) production (via methanogenesis), which could decrease long-term carbon storage and climate change mitigation benefits of wetlands. Microbial functions associated with the delivery of ecosystem services have the potential to be managed to enhance beneficial wetland services (Peralta, Stuart, et al. 2014). To achieve microbial management, a deeper understanding of the controls on wetland microbial ecosystem functions is needed.

To produce cellular energy, adenosine triphosphate (ATP), microorganisms catalyze a series of oxidation-reduction (redox) reactions. Aerobic respiration yields the greatest amount of energy and is expected under dry conditions, but as water fills soil pore spaces, diffusion of oxygen (O_2) into the soil matrix decreases, causing a shift to a reducing environment (Truu, Juhanson, and Truu 2009; Mitsch et al. 2013). Reducing environments favor anaerobic respiration in which other molecules such as nitrate (NO_3^-), manganese, ferric iron, sulfate, and

carbon dioxide (CO_2) are used as terminal electron acceptors (Burgin et al. 2011). As soil moisture increases, O_2 availability and soil redox potentials decrease, which corresponds to a shift in available electron acceptors (Truu, Juhanson, and Truu 2009). Redox potentials measured between +600 and +250 mV are considered oxidative conditions, while redox potentials measured from +250 to -400 mV are considered reducing conditions (Truu, Juhanson, and Truu 2009). Therefore, measuring soil redox potential is useful for predicting which biogeochemical processes are likely to be carried out by soil microbes.

To manage microbial functions in support of nitrogen removal and retention but with decreased CH_4 production, a better understanding of the extent to which the presence of vegetation and changes in hydrology (e.g., flooding, drying) affect microbial communities is needed. Complex interactions between abiotic factors, such as soil physicochemical properties, redox status, and nutrient availability, and biotic factors, including the abundance of vegetation and microbial community structure, influence microbial functions to varying degrees. A microbial community is composed of many taxa with varying physiologies that respond differently to changes in the local environment (Mentzer, Goodman, and Balser 2006; Nygaard and Ejrnæs 2009). Particular microbes may be more adapted to specific hydrologic conditions in their environment, where only a subset of microbial taxa can persist in response to frequent changes in soil moisture (Peralta, Ludmer, et al. 2014; Truu, Juhanson, and Truu 2009). However, unexpected microbial responses can also occur due to dormancy of soil bacterial taxa (Lennon and Jones 2011; Rocca et al. 2015). As such, hydrologic changes in wetlands due to drought, draining, and re-wetting cause shifts in soil redox potentials and microbial community composition and metabolism, which can influence the relative rates of anaerobic processes such

as denitrification and methanogenesis (Kim et al. 2008; Truu, Juhanson, and Truu 2009; Peralta, Ludmer, et al. 2014).

If drying and re-wetting events are periodic, a cycle of activity and dormancy can maintain high microbial diversity compared to more stable environmental conditions (Peralta, Ludmer, et al. 2014). For example, denitrifiers are facultative anaerobes and can use O_2; however, under anoxic conditions, they switch to reducing NO_3^- to nitrous oxide (N_2O) and dinitrogen (N_2) gas during respiration (Mitsch and Gosslink 2007). In addition, methanogens are dominant in the most anoxic conditions, such as flooded wetlands, and are responsible for converting CO_2 to CH_4 (Mitsch and Gosslink 2007). Fluctuating hydrologic conditions can shift the microbial community to one that can only tolerate transitional zones. As hydrologic changes occur, oxic-anoxic interfaces provide environmental conditions that sometimes support methanotrophs, which transform CH_4 to CO_2, and denitrifiers (McDonald and Murrell 1997; Mitsch and Gosslink 2007; Conrad 2009). Therefore, the availability of electron acceptors (e.g., O_2, NO_3^-) in the soil environment influences the relative abundance of microbial functional groups (i.e., subset of microbes capable of using a suite of electron acceptors) and rates and types of microbial processes.

While hydrology is a primary determinant of soil redox potential, plants also modify the soil environment. The soil microenvironments that are in contact with plant roots are hotspots of microbial activity due to plant-mediated transport of nutrients, O_2, and carbon belowground (Kuzyakov 2010; Philippot et al. 2013; Chanton 2005). Plants can also transport CH_4 aboveground through aerenchyma in shoots. Radial O_2 loss from plant roots can increase soil redox potentials around the root zone, producing microenvironments that support aerobic microbial processes (Chanton 2005). Additionally, vegetation can alter soil redox potentials by

121 facilitating transport of O_2 into root zones (Chanton 2005; Sundberg et al. 2007) and transporting
122 CH_4 from root zones into the atmosphere (Carmichael et al. 2014; Hu et al. 2015).
123 The aim of this study is to provide insight into how the duration of hydrologic change
124 (i.e., sustained dry, interim dry/wet, sustained wet), and the presence of vegetation in wetland
125 soils change the structure of the microbial community, redox conditions, and greenhouse gas
126 (GHG) production. We hypothesize that dry and dry/wet transition conditions will support
127 similar microbial communities, but that redox potentials and GHG production rates will differ
128 between manipulated hydrologic treatment conditions. We expect that dry conditions with and
129 without vegetation will support higher redox potentials (i.e., oxidative conditions) and a higher
130 rate of CO_2 production with some N_2O production but little or no CH_4 production. We expect
131 this because dry and transition conditions should support similar communities of facultative
132 anaerobes that can switch between respiration pathways depending on current soil saturation
133 levels. Additionally, in dry conditions, soils are already aerated, so plant-mediated gas transport
134 belowground should not alter redox potentials. However, in fluctuating wet conditions, we
135 expect that redox conditions will shift between oxidative and reducing conditions due to soil
136 saturation. Also, plant presence is expected to increase redox potentials during saturated periods,
137 due to plant-mediated gas transport belowground, compared to treatments where vegetation is
138 absent. Due to lower O_2 levels when saturated conditions are present, we expect decreased CO_2
139 production but increased N_2O production with plants due to plant stimulation of denitrification
140 via organic matter inputs and elevated O_2 supporting nitrification to supply NO_3^- to denitrifiers
141 (Alldred and Baines 2016). Additionally, in the presence of plants and in dry or interim
142 conditions, we expect CH_4 production to be lower due to methanogens being obligate anaerobes.
143 Flooded conditions will support different microbial communities than dry or fluctuating

144 environments due to consistently low redox potentials (i.e., reducing conditions), resulting in the
145 highest rates of CH_4 production and complete denitrification rates since these are both anaerobic
146 processes. Although other studies (Carmichael et al. 2014; Hu et al. 2015) have found increased
147 methanogenesis in the presence of some plant species, in the present study, we expect that soils
148 with plants will have lower CH_4 production compared to flooded soils without plants. This is
149 expected due to O_2 transport from the roots, which supports aerobic methanotrophic microbial
150 taxa that consume CH_4.

151 To test these hypotheses, we conducted a mesocosm experiment in which we
152 manipulated hydrology (i.e., dry, interim, and wet) and the presence of plants in soils collected
153 from different hydrologic histories (i.e., dry, wet/dry transition, and saturated wet zones) within a
154 restored coastal plain wetland. We measured soil nutrient concentrations, redox potentials, GHG
155 fluxes, and characterized soil microbial communities using 16S rRNA gene amplicon
156 sequencing. By simulating acute differences in hydrologic states, the addition of plants, and the
157 maintenance of soil structure, we were able to link microbial-scale changes to ecosystem-level
158 processes.

159

160 **Methods**

161 *Study site*

162 We collected soil samples from the Timberlake Observatory for Wetland Restoration
163 located in the Albemarle Peninsula in Tyrell County, North Carolina (35°54’22” N 76°09’25”
164 W; Figure 1). Previously described by Ardón et al., the field site is part of the Great Dismal
165 Swamp Mitigation Bank, LLC, which is a 1,700 ha wetland consisting of 420 ha of mature
166 forested wetland, 787 ha of forested wetland, 57.2 ha of drained shrub-scrub, and 440 ha of

agricultural fields restored to wetland habitat in 2007 (Ardón et al. 2010; 2013; Morse, Ardón, and Bernhardt 2012). A major portion of the restoration effort was to remove drainage ditches and plant 750,000 saplings including *Taxodium distichum, Nyssa* spp., *Salix nigra, Fraxinus pennsylvanica, and Quercus* spp. (Morse, Ardón, and Bernhardt 2012). A more recent survey indicates that the dominant plant species at the site is *Juncus effusus* L., along with *Euthamia caroliniana* (L.) Greene ex Porter & Britton, *Solidago fistulosa* Mill., and *Scirpus cyperinus* (L.) Kunth (Hopfensperger et al. 2014). The site is connected to the Albemarle Sound via the Little Alligator River, and the site's position in the landscape increases the potential for saltwater intrusion to occur. In addition, salinity in the sound ranges from 0-7 psu and up to 12 psu during drought years (Ardón et al. 2013). Even though there is little elevation change (-1 m to 2 m) across the restored wetland, there is a hydrologic gradient, which is driven by the position of the water table and represents upland dry, saturated wet, and transition dry/wet sites (Hopfensperger et al. 2014).

Mesocosm experimental design

We used a mesocosm approach to assess the changes in the soil microbial community, redox potentials, and GHG production due to hydrologic changes and vegetation. We set up a mesocosm experiment using soil blocks collected from three sites within the Timberlake Observatory for Wetland Restoration field site. Soils were collected from the restored portion of the site (12 years post-restoration), which had been used as agricultural fields for several decades prior to restoration (Ardón et al. 2010). We collected soils that represented three different hydrologic zones on the inflow side of the site at the following coordinates: 35°53'45.3"N 76°09'57.5" W (dry), 35°53'44.8" N 76°09'57.1" W (dry/wet transition or interim), and

35°53'44.3" N 76°09'56.0" W (wet). Six intact soil blocks (25 cm × 25 cm × 20 cm deep) were cut out from each of the three sites using landscaping knives and shovels. Soil history was determined by water table levels at the time of collection (dry = 20 cm, interim = 10 cm, and wet = 0 cm below surface level). Soil blocks were contained in dark plastic containers of the same dimensions as the soil blocks (Figure 1). To manipulate hydrology within the mesocosm, vinyl tubing was inserted 3 cm from the bottom of the mesocosm container on each side and connected to a 1 L water bottle (Figure 1). Water levels inside the mesocosm were maintained by filling the 1 L bottle to the desired height using rainwater collected from a cistern. To manipulate the presence of vegetation, the mesocosm was divided in half and separated by a root screen (20 µm stainless steel mesh). On one side, plants were allowed to grow during the experiment, while the 'no plant' side was maintained by careful removal of above- and belowground plant biomass. Finally, 4" schedule 40 polyvinyl chloride (PVC) collars were inserted 5 cm below the surface as a sampling base for GHG chambers (described in subsection *GHG fluxes*). The mesocosm experiment was housed at the East Carolina University (ECU) West Research Campus (Greenville, NC) under a covered hoop house with shade cloth, which prevented precipitation and allowed 60% light into the hoop house. Soils were collected on April 1, 2016, and prepared on May 29, 2016. Experimental mesocosm sampling commenced on June 13, 2016, and concluded on August 11, 2016. Temperatures ranged from 22.7 °C ± 1.5 to 30.8 °C ± 1.4 during the experimental sampling period. Because the hoop house was in a wetland approximately 100 miles from the field site, within the same physiographic region, the temperature and relative humidity in the hoop house would have closely resembled field conditions. Blocking precipitation was essential for the controlled manipulation of hydrologic conditions.

212 Two weeks after installing PVC collars and setting up the plant treatment, we started
213 hydrologic treatments. Hydrologic manipulation occurred over eight weeks to allow for multiple
214 dry/wet transitions for the interim treatment. Mesocosms exposed to wet conditions were flooded
215 by overhead watering and maintained using water reservoirs filled to maximum container height
216 (18 cm). Mesocosms exposed to dry conditions were maintained using water reservoirs filled to a
217 depth of 5 cm. The dry/wet (interim) treatments fluctuated between flooded and dry conditions,
218 as described above, every two weeks, starting with a wet treatment and ending with a dry
219 treatment. We measured soil redox status and microbial community composition at the beginning
220 and end of the eight-week experiment. Additionally, we measured GHG fluxes every two weeks,
221 starting two weeks after initiating the hydrologic treatments. Finally, at the end of the eight-week
222 experiment, we collected soils for physiochemical analyses: soil moisture, pH, total carbon, total
223 nitrogen, extractable ammonium (NH_4^+) and NO_3^-, phosphorus, potassium, magnesium, sulfur,
224 iron, manganese, and organic matter concentrations (described in subsection *Soil physiochemical*
225 *characteristics*).
226
227 *Measuring integrated soil redox status*
228 We measured soil redox status at the beginning and end of the hydrologic experiment
229 using Indicator of Reduction in Soils (IRIS) tubes (InMass Technologies (Jenkinson and
230 Franzmeier 2006), Figure 2, Appendix S1: Figure S1). The IRIS tubes are constructed from 1/2"
231 schedule 40 PVC pipe coated in iron oxide (Fe(III)) paint (Rabenhorst 2008). When exposed to
232 oxidative conditions, Fe(III) appears as an orange-red paint; but when exposed to anoxic
233 conditions, Fe(III) is reduced to Fe(II) which dissolves in solution and appears as a clearing
234 (white) on the tube (Jenkinson and Franzmeier 2006; Rabenhorst 2008). At the beginning of the

experiment, two IRIS tubes (12 cm depth) were installed in each mesocosm: one on the plant side and one on the bare soil side. The IRIS tubes were incubated in mesocosm conditions for two weeks before removal and analysis. After we removed the IRIS tube, a non-coated PVC pipe was used to fill the hole. Two weeks prior to the end of the experiment, the non-coated PVC pipe was removed and replaced with a new IRIS tube to measure soil redox status at the end of the experiment.

We quantified the surface area of Fe(III) paint removed from IRIS tubes using *ImageJ* (v1.48 (C. A. Schneider, Rasband, and Eliceiri 2012)). First, we imaged the entire tube by taking four pictures and then stitched the photos into a composite using *GIMP2* (v2.8.14) photo editing software (Kimball et al. 2014). Next, we identified areas of artificial paint removal, that is, scratches from installing or removing tubes, and manually filled these pixels. Then, using *ImageJ* (C. A. Schneider, Rasband, and Eliceiri 2012), we converted all colored pixels to black. We compared the number of white pixels to the total pixels to determine the percentage of paint removed. Interpretation of redox status is based on the percent paint removed from a 10 cm section of tubing and summarized as follows: 0% not reducing, 1-5% probably not reducing, 5-10% possibly reducing, 10-25% and >25% definitely reducing (Rabenhorst 2008). For regression analysis of GHG fluxes as a function of redox status, the percent of paint removed was treated as a continuous variable to represent redox status.

Soil physicochemical characteristics

Soil properties were determined from soils collected during the destructive sampling of mesocosms at the end of the experimental duration. We collected six soil cores (3 cm diameter, 10 cm depth) from each side of the box (i.e., plant and no plant) and combined cores collected

258 from one side into a composite sample (i.e., one plant composite and one no plant composite),
259 passed soils through a 4 mm sieve, and homogenized samples prior to subsampling for soil
260 analyses. For each sample, we measured gravimetric soil moisture by drying 20-30 g of field-
261 moist soil at 105 °C for at least 24 hours. Approximately 5 g of field moist soil was extracted
262 with 45 ml of 2 M KCl, and extractable NH_4^+ and NO_3^- ions were colorimetrically measured
263 using a SmartChem 200 auto analyzer (Unity Scientific, Milford, Massachusetts, USA) at the
264 East Carolina University Environmental Research Laboratory. To determine total carbon and
265 total nitrogen (TC, TN), a subsample of air-dried soil was finely ground and sieved through a
266 500 µm mesh and analyzed using an elemental analyzer (2400 CHNS Analyzer; Perkin Elmer,
267 Waltham, Massachusetts, USA) at the Environmental and Agricultural Testing Service
268 Laboratory, Department of Crop and Soil Sciences, North Carolina State University. A second
269 subsample of air-dried soil was sent to Waters Agricultural Laboratories, Inc. (Warsaw, NC) and
270 analyzed for pH, phosphorus, potassium, magnesium, sulfur, manganese, iron, and humic matter,
271 using standard Mehlich III methods (Mehlich 1984; Mylavarapu et al. 2014).
272
273 *Greenhouse gas (GHG) fluxes*
274 We examined the effects of hydrology and vegetation on GHG production. We measured
275 GHG fluxes on June 13, 2016, two weeks after hydrologic treatments were established, and then
276 every two weeks until August 11, 2016, for a total of five sampling events. The GHG collection
277 chambers were 20 cm in height with a diameter of 8.25 cm and constructed from clear acrylic
278 tubing. Since GHG samples were captured using clear chambers versus opaque chambers, GHG
279 measurements represent total GHG fluxes and not just soil respiration due to microbial activity.
280 Chambers were sealed on one end with silicon and a pipe cap with a 33 mm septum installed as a

281 gas sampling port. At the time of sampling, chambers were placed on top of preinstalled PVC
282 collars, and the seals were taped to prevent diffusion from the seam (Hoffmann et al. 2018). A
283 gas sample was collected from chambers at four time points: 30 minutes, 60 minutes, 120
284 minutes, and 180 minutes after chamber attachment. Initial ambient (T_0) samples were not
285 obtained before chamber closure. Instead, they were collected from the mesocosm incubation
286 field site at the ECU West Research Campus as part of a 16-month effort to sample coastal plain
287 wetland GHGs, spanning from August 2021 to December 2022. Monthly average ambient GHG
288 concentrations were calculated and used to represent the T_0 concentration for mesocosm flux
289 measurements within each corresponding month. To collect gas samples, we used a needle
290 attached to a 20 mL syringe, mixed headspace gas three times by pulling and depressing the
291 plunger, and then collected 20 mL of sample. The collected gas sample was equally distributed
292 between two 3 mL glass Exetainer vials (Lampeter, Wales, UK) fitted with screw top and dual
293 layer septa. Samples were stored upside down at room temperature in a dark location and were
294 analyzed within 96 hours of collection. We analyzed GHG concentrations using a Shimadzu gas
295 chromatograph (GC-2014) fitted with an electron capture detector to detect N_2O and a flame
296 ionization detector with a methanizer to measure CH_4 and CO_2. Calibration standards for June 13
297 and June 28, 2016, contained 0, 120, 240, 360, and 480 CO_2 parts per million (ppm); 0, 1, 2, 3, 4,
298 and 5 CH_4 ppm; 0, 0.2, 0.4, 0.6, 0.8, and 1 N_2O ppm. Calibration standards for July 11, Jul 25,
299 and August 11, 2016, contained 0, 120, 480, 1200, 2400, and 3000 CO_2 ppm; 0, 1, 4, 20, 40, and
300 50 CH_4 ppm; 0, 0.2, 0.8, 20, 40, and 50 N_2O ppm. Monthly ambient samples collected from
301 August 2021 to December 2022 were calibrated against standards containing CO_2 at 0, 120, 240,
302 360, 480, 600, 1200, 1800, 2400, and 3000 ppm; CH_4 at 0, 1, 2, 3, 4, 5, 10, 20, 30, 40, and 50
303 ppm; and N_2O at 0, 0.2, 0.4, 0.6, 0.8, 1, 10, 20, 30, 40, and 50 ppm. If a sample measured above

304 the calibration curve, we diluted the sample, remeasured the concentration, and accounted for the
305 dilution factor when calculating the final concentrations.

306 We calculated GHG fluxes using the *gasfluxes* package implemented in the R Statistical
307 Environment and RStudio (RStudio 2024.12.0+467, Rv4.4.2) (Fuss and Hueppi 2024; R Core
308 Team 2024). Using *gasfluxes*, the best model fit among HMR, robust linear, and linear was
309 selected for each flux (Appendix S2).

310 *Bacterial and archaeal community analyses*

311 We assessed the soil microbial community composition at the beginning of the
312 experiment ('start', based on soils collected from the IRIS tube installation) and at the end of the
313 experiment ('final', based on soils collected during destructive sampling). We collected 'final'
314 soil samples using a standard soil probe (3 cm diameter, 10 cm depth) from the same location
315 that we collected GHG samples. We extracted genomic DNA from the soils using the Qiagen
316 DNeasy PowerSoil Kit and diluted the DNA to 20 ng/µL. This genomic DNA was used as
317 template in PCR reactions and used barcoded primers (bacterial/archaeal 515FB/806R primer
318 set) originally developed by the Earth Microbiome Project to target the V4 region of the bacterial
319 16S subunit of the ribosomal RNA gene (Caporaso et al. 2012; Apprill et al. 2015; Parada,
320 Needham, and Fuhrman 2016). For each sample, three 50 µL PCR libraries were prepared by
321 combining 35.75 µL molecular grade water, 5 µL Amplitaq Gold 360 10x buffer, 5 µL $MgCl_2$
322 (25 mM), 1 µL dNTPs (40mM total, 10mM each), 0.25 µL Amplitaq Gold 360 polymerase, 1 µL
323 515 forward barcoded primer (10 µM), 1 µL 806 reverse primer (10 µM), and 1 µL DNA
324 template (10 ng μL^{-1}). Thermocycler conditions for PCR reactions were as follows: initial
325 denaturation (94 °C, 3 minutes); 30 cycles of 94 °C for 45 seconds, 50 °C for 30 seconds, 72 °C
326 for 90 seconds; final elongation (72 °C, 10 minutes). The triplicate 50 µL PCR libraries were

327 combined and then cleaned using the Axygen® AxyPrep Magnetic (MAG) Bead Purification Kit
328 (Axygen, Union City, California, USA). Cleaned PCR products were quantified using the
329 QuantIT dsDNA BR assay (Thermo Scientific, Waltham, Massachusetts, USA) and diluted to a
330 concentration of 10 ng/µL before pooling the libraries at an equimolar concentration of 5 ng/µL.
331 We sequenced the pooled libraries using the Illumina MiSeq platform using paired-end reads
332 (Illumina Reagent Kit v2, 500 reaction kit) at the Indiana University Center for Genomics and
333 Bioinformatics Sequencing Facility.

334 Sequences were processed using the *mothur* (v1.42.0) MiSeq pipeline (Kozich et al.
335 2013; Schloss et al. 2009). We assembled contigs from the paired-end reads, quality trimmed
336 using a moving average quality score (minimum quality score 35), aligned sequences to the
337 SILVA rRNA database (v132) (Quast et al. 2013), and removed chimeric sequences using the
338 VSEARCH algorithm (Rognes et al. 2016). We created operational taxonomic units (OTUs) by
339 first splitting sequences based on taxonomic class and then binning them into OTUs based on
340 97% sequence similarity. Since amplicon sequencing was conducted using short reads (250 bp)
341 and not assembled genomes, we used an OTU-based 3% distance threshold to avoid splitting the
342 same bacterial genome into distinct clusters (using amplicon sequence variant (ASV) of a single
343 base difference). An OTU-based approach also limits over-inflated numbers of ASVs introduced
344 by PCR bias and sequencing errors (Schloss 2021). In addition, employing an OTU- or ASV-
345 based approach is known to result in similar broadscale community composition patterns
346 (Glassman and Martiny 2018).

347

348 *Shotgun metagenomic analyses*

349 Based on amplicon sequencing, we identified a subset of samples representing the most
350 distinct microbial communities for shotgun metagenomic sequencing. A Description of sample
351 processing and metagenomic sequencing can be found in Peralta et al. (2020). Briefly, we chose
352 a set of baseline and post-flooding/drying treatment samples. We sourced mesocosm baseline
353 conditions from relatively drier field locations (water level at about -20 cm, n = 4) and relatively
354 wetter plots (water level at about 0 cm, n = 4). At the end of the eight-week experiment, we
355 selected a subset of samples from the hydrologic treatments (prolonged drying or wetting only)
356 and plant treatments (presence or absence of vegetation) (n = 16). After genomic DNA extraction
357 using the Qiagen DNeasy PowerMax soil kit, samples were sent to the U.S. Department of
358 Energy (DOE) Joint Genome Institute (JGI) for sequencing and analysis (GOLD study ID
359 Gs0142547 and NCBI BioProject accession number PRJNA641216). Plate-based DNA library
360 preparation and subsequent Illumina sequencing, according to published protocols (Peralta et al.
361 2020), resulted in 583.2 Gbp of raw sequence data. Raw data were processed using the DOE JGI
362 Metagenome Annotation Pipeline IMG/M v.5.0.9 (Chen et al. 2017; Huntemann et al. 2016;
363 Markowitz et al. 2014).
364 From the metagenomes, we curated functional gene sets using IMG/M's integrated Kyoto
365 Encyclopedia of Genes and Genomes (KEGG) module list. For statistical analyses, we focused
366 on the following four functional gene sets associated with biogenic greenhouse gas
367 concentrations of N_2O, CH_4, and CO_2: (1) Denitrification (KEGG Module M00529), (2)
368 Methanogen (M00617), (3) Central Carbohydrate Metabolism (M00001-M00011, M00307-
369 M00309, M00580, and M00633), and (4) Prokaryotic Cytochrome C Oxidase (CcO) (M00155).
370
371 *Statistical Analyses*

372 All statistical analyses were performed in the R statistical environment (RStudio
373 2024.12.0+467, Rv4.4.2) (R Core Team 2024). Prior to multivariate statistical analyses, we
374 normalized sample-to-sample variation in sequence depth by taking the relative abundance of
375 each OTU: dividing the count of each OTU by the total number of OTUs for each soil
376 community. OTU data were then rarefied using *vegan::rrarefy*, producing randomly sampled
377 subsets of OTUs with each sample having an equal number of unique OTUs (Oksanen 2015).
378 Likewise, functional gene counts were converted to relative abundance by dividing the count of
379 each functional gene by the total number of functional gene counts in each respective functional
380 gene category. We examined beta diversity by visualizing bacterial community responses to
381 hydrologic history (field conditions), hydrologic treatment (contemporary dry/wet treatments),
382 and plant presence/absence using principal coordinates analysis (PCoA) of bacterial community
383 composition based on Bray-Curtis dissimilarity. We also used PCoA to visualize composition
384 (Bray-Curtis dissimilarity) of functional gene categories according to hydrologic history,
385 hydrologic treatment, and plant presence/absence. We used permutational multivariate analysis
386 of variance (PERMANOVA) to determine differences between bacterial communities among
387 hydrologic history, hydrologic treatment, and plant presence. Hypothesis testing using
388 PERMANOVA was performed using the *vegan::adonis* function (Oksanen 2015). Unique taxa
389 representing each hydrologic history and hydrologic treatment were determined by Dufrene-
390 Legendre indicator species analysis using the *labdsv::indval* function (Roberts 2023). Finally,
391 soil parameters were compared against bacterial community and functional patterns (based on
392 Bray-Curtis dissimilarity) using the *vegan::envfit* function (Oksanen 2015). Soil parameters with
393 $p \leq 0.05$ were represented on the PCoA plot of 16S rRNA community composition as vectors
394 scaled by their correlation to microbial community patterns. The GHG fluxes and soil parameters

with $p \leq 0.1$ were plotted as vectors, scaled by their correlation, on PCoA plots of functional gene composition.

We constructed linear mixed effects models with sampling plot (mesocosm) and sampling date as random effects to determine the importance of the fixed effects of hydrologic history (field conditions), hydrologic treatment (contemporary dry/wet treatments), and plant presence on GHG fluxes using the *lme4* R package (Bates et al. 2015). Then, we used Akaike's Information Corrected Criterion (AICc) model comparisons, which adjust for small sample size, against the null model to determine which simplest combination of fixed effects (hydrologic history, hydrologic treatment, and plant presence) is needed to explain the most variance in GHG fluxes (Hurvich and Tsai 1993; Gorsky et al. 2019). We compared individual fixed effects and the combination of those fixed effects. We did not use the interaction between the fixed effects hydrologic history and hydrologic treatment because combinations would have resulted in a sample size of $n = 2$ for each group. Lastly, to determine the proportion of variance explained by fixed effects (marginal) and the complete model (conditional), we used the *MuMIn* R package (Gorsky et al. 2019; Bartoń 2025).

While linear mixed effects models are robust to departures from normality (Schielzeth et al. 2020), traditional ANOVAs and t-tests are less so (Blanca et al. 2017; Havlicek and Peterson 1974). To accommodate extreme outliers and lack of normality, we used nonparametric statistics to test for differences in GHG fluxes among hydrologic treatments and plant presence/absence. We used Wilcoxon Rank Sum tests to evaluate differences in GHG fluxes among plant versus no plant groups. To accommodate repeated measures without pseudoreplication, Wilcoxon Rank Sum tests were blocked by sampling date. We used Kruskal-Wallis tests to examine differences in GHG fluxes among the three hydrologic treatments (dry, interim, and wet). To accommodate

418 repeated measures, Kruskal-Wallis tests were grouped by sampling date. If the Kruskal-Wallis
419 test for a sampling date revealed differences among treatment groups ($p \leq 0.05$), we then
420 performed pairwise comparisons using the Dwass, Steel, Critchlow, and Fligner (SDCFlig) test
421 with a Monte Carlo distribution (G. Schneider, Chicken, and Becvarik 2023).
422 To assess microbial community structure and function relationships, we examined the
423 relationship between GHG fluxes and microbial community/functional Bray-Curtis dissimilarity
424 matrices using distance-based partial least squares regression (DBPLSR) in the *dbstats* R
425 package (Boj et al. 2024). Finally, we used the *mantel* function in the *vegan* R package (Oksanen
426 2015) to examine the relationship between the soil properties (redox, percent moisture, pH,
427 NH_4^+, total soil C, total soil N, phosphorus ppm, potassium ppm, magnesium ppm, sulfur ppm,
428 iron ppm, manganese ppm, and percent humic matter), GHG fluxes, and microbial community
429 composition.
430
431 **Data Availability**
432 All code and data used in this study are in a public GitHub repository
433 (https://github.com/PeraltaLab/WetlandMesocosm_GHG_Timberlake) with a Zenodo DOI
434 (https://doi.org/10.5281/zenodo.15528281). Raw amplicon sequence files can be found at NCBI
435 SRA BioProject ID PRJNA636184, and metagenome sequence files can be found at NCBI
436 SRA BioProject ID PRJNA641216.
437
438 **Results**
439 Soil mesocosms sampled from the Timberlake Observatory for Wetland Restoration, in
440 three distinct hydrologic conditions (dry, interim, wet) (Figure 1), were subjected to eight weeks

441 of hydrologic and plant presence/absence treatments (Figure 1). The three levels of eight-week
442 hydrologic treatments were: (1) flooded for eight weeks, (2) dry for eight weeks, and (3) interim,
443 i.e., two weeks flooded alternating with two weeks dry for a total of eight weeks. Each box was
444 separated by a stainless mesh divider, with plants allowed to grow on one side and plants
445 removed on the other side (Figure 1).
446
447 *Characterization of soil physical-chemical properties*
448 There was little variability in soil properties across main effects (hydrologic history,
449 hydrologic treatment, plant presence), except for notable differences in soil moisture between
450 plant treatments within dry and wet hydrologic treatments (Table 1). In addition, NO_3^-N
451 concentrations were below detection limits in samples with plants, but concentrations were
452 measurable in samples without plants (Table 1). Soil redox status as measured by IRIS tube
453 analysis revealed that soils experiencing dry and interim treatments were not reducing (0% iron
454 oxide paint removed), while soils in wet treatments were reducing (average 40%, range 27-67%
455 paint removed) (Figure 2). In wet treatments, plant presence enabled soil redox status to decrease
456 to a lesser degree (average 38%, range 27%-60% paint removed) than when plants were absent,
457 but soils were still considered reducing (Figure 2, Appendix S1: Figure S1).
458
459 *Plant and soil redox effects on greenhouse gas fluxes*
460 *Methane (CH_4)*
461 Wet hydrologic treatment and no plants produced the highest CH_4 fluxes and the greatest
462 variability between samples (10.31 ± 45.54 mg CH_4 m^{-2} h^{-1}, $\bar{x} \pm SD$, Appendix S1: Table S1).
463 Interim hydrologic treatment with plants produced the second highest mean CH_4 fluxes (2.56 mg

464 CH_4 m^{-2} h^{-1}), but interim hydrology with no plants produced the lowest mean CH_4 fluxes (0.75
465 mg CH_4 m^{-2} h^{-1}; Appendix S1: Table S1). Excluding interim hydrology, the order of mean CH_4
466 fluxes from greatest to least is wet and no plants, dry and no plants, wet with plants, and dry with
467 plants (Appendix S1: Table S1). When comparing plant vs. no plant CH_4 fluxes at each of the
468 five timepoints, no differences were detected, except for during the second timepoint on June
469 28th, where CH_4 concentrations were greater in the presence of plants than in the absence of
470 plants (Figure 3, Appendix S1: Table S2). There were differences in CH_4 fluxes in the
471 hydrologic treatment groups in three of the five timepoints (Figure 4, Appendix S1: Table S3).
472 The wet treatment produced greater CH_4 fluxes than the dry treatment throughout the middle
473 three timepoints (June 28th through July 25th), and differences in wet vs. interim and dry vs.
474 interim were observed but did not persist throughout the experiment (Figure 4, Appendix S1:
475 Table S3). The null linear mixed-effects model with random effects only (sample mesocosm and
476 date) was the most plausible (ΔAICc = 0), with an AICc weight of 0.37 (Appendix S1: Table
477 S4). The fixed effects of plant presence/absence, hydrologic history, and hydrologic treatment
478 explained little variance in CH_4 fluxes (Appendix S1: Table S4).
479
480 *Carbon dioxide (CO_2)*
481 CO_2 fluxes were greater in no plant mesocosms compared to plant mesocosms, except
482 during the fourth timepoint on July 25th (Figure 3, Appendix S1: Table S2). CO_2 fluxes in the dry
483 hydrologic treatment were greater than CO_2 fluxes in the interim and wet treatments during two
484 out of five timepoints (Figure 4, Appendix S1: Table S3). The linear mixed effects model, which
485 included the interactive effects of hydrologic treatment and plant presence/absence, was the most
486 plausible (ΔAICc = 0), based on an AICc weight of 1.00 (Appendix S1: Table S4). The most

plausible model explained 49% of the variance in CO_2 fluxes (conditional R^2, Appendix S1: Table S4). In comparison, the fixed effect of plant presence/absence explained 12% of the variance in CO_2 fluxes, and hydrologic treatment and hydrologic history explained 19% and 1%, respectively (Appendix S1: Table S4).

Nitrous oxide (N_2O)

The N_2O fluxes were near zero in all hydrologic and plant treatments (range: -4.61 – 2.88 mg N_2O m^{-2} h^{-1}) (Figure 3, Figure 4). On July 11th and July 25th, no plant N_2O fluxes exceeded plant N_2O fluxes (Figure 3, Appendix S1: Table S2). The N_2O fluxes were similar among hydrologic treatments, except for lower fluxes in interim hydrology on June 13th (Figure 3, Appendix S1: Table S2). The model with plant and hydrologic treatment additive effects was most plausible (ΔAICc = 0), based on an AICc weight of 0.25 (Appendix S1: Table S4). The most plausible model (plant + hydrologic treatment) explained 43% of the variance (conditional R^2), while the fixed effect of plant explained 1.6% of the variance, and hydrologic treatment explained 1.5% of the variance (Appendix S1: Table S4).

Relationship between soil redox conditions and GHG fluxes

We used linear regression to examine the relationship between soil redox status (represented by the percent of paint removed from IRIS tubes) and GHG fluxes. At the start of the experiment, the CH_4 fluxes had a weak positive relationship to redox status ($F_{34} = 3.14$, $R^2 = 0.06$, $p = 0.09$, Appendix S1: Table S5, Figure S2). At the end of the experiment, the CO_2 fluxes had a negative relationship with redox conditions ($F_{34} = 6.90$, $R^2 = 0.14$, $p = 0.01$, Appendix S1:

Table S5, Figure S2). The N_2O fluxes were not significantly related to redox conditions throughout the experiment (Appendix S1: Table S5, Figure S2).

Patterns in microbial community composition

Sequencing efforts returned 1,570,135 reads and 35,897 OTUs before removing low-abundance sequences occurring less than 10 times or 0.01% in all samples. After removing low-abundance sequences, 1,505,797 reads representing 7,026 OTUs were retained after filtering. Within pre-filtering OTUs, 15,582 occurred once, and 5,536 occurred twice in all samples. All samples were rarefied to 23,528 reads since this was the lowest read count among all samples.

Bacterial and archaeal community composition clustered by hydrologic treatment within hydrologic history (Figure 5). PCoA axis 1 explained 25% and PCoA axis 2 explained 11% of microbial community variance (Figure 5). We observed that hydrologic history (PERMANOVA, $F_{2, 35} = 7.562$, $R^2 = 0.305$, $p = 0.001$) and hydrologic treatment (PERMANOVA, $F_{2, 35} = 2.605$, $R^2 = 0.110$, $p = 0.002$) explained variance in microbial community patterns (Figure 5, Appendix S1: Table S6). In contrast, microbial community composition was similar in the presence or absence of plant communities (PERMANOVA, $F_{1, 35} = 0.698$, $R^2 = 0.102$, $p = 0.824$, Appendix S1: Table S6). In addition, sulfur concentrations were correlated to soil microbial communities from the wet hydrologic history, pH levels were correlated to microbial communities from the interim hydrologic history, and total soil C and N were correlated to microbial communities from the dry hydrologic history (Figure 5). Also, overall patterns in microbial composition and soil properties were significantly correlated (Mantel $r = 0.384$, $p = 1.0 \times 10^{-4}$, Appendix S1: Table S7).

531 Indicator species analysis of the top 2.5% of OTUs (by relative abundance at a
532 significance level of $p \leq 0.01$) revealed that 34 OTUs, 21 OTUs, and 38 OTUs represented dry,
533 interim, and wet hydrologic histories, respectively (Appendix S1: Table S8). The bacterial phyla
534 *Acidobacteria* (Gp1, Gp2, Gp3, and Gp6) (24%) and *Proteobacteria* (*Alpha*-, *Beta*-, *Delta*-, and
535 *Gammaproteobacteria*) (30%) represented communities from dry hydrologic histories, while the
536 bacterial phyla *Acidobacteria* (Gp1, Gp10, Gp3, and Gp7) (33%) and *Proteobacteria* (Alpha-,
537 Beta-, and *Deltaproteobacteria*) (29%) represented communities from interim hydrologic
538 histories (Appendix S1: Table S8). Soils from wet hydrologic histories were represented by
539 *Acidobacteria* (Gp1, Gp2, Gp3) (38%) and *Proteobacteria* (Alpha-, Delta-, and
540 *Gammaproteobacteria* (21%) (Appendix S1: Table S8). Finally, microbial taxa putatively
541 associated with methane cycling including the archaeal genera *Methanobacterium* and the
542 bacterial genera *Methylocystis* and *Syntrophobacter* were unique to microbial communities from
543 wet hydrologic histories (Appendix S1: Table S8). Fewer indicator OTUs were identified for
544 hydrologic treatments (6 OTUs, and 9 OTUs, for interim, and wet hydrologic treatments,
545 respectively, Appendix S1: Table S9). Only one indicator OTU was found in common among
546 hydrologic histories and hydrologic treatments. Interestingly, this shared OTU, *Reyranella*, was
547 indicative of both dry historical conditions and wet hydrologic treatment conditions.
548
549 *Patterns in functional gene composition*
550 Following quality control and filtering of raw metagenomic sequencing data, annotation
551 and gene calling resulted in 600,507 ± 172,049 ($\bar{x} \pm SD$) annotated contigs per sample. An
552 average of 998,604 ± 307,431 gene features per sample were identified. Of the identified gene
553 features, an average of 232,809 ± 70,486 KEGG features per sample were identified. Among the

554 four curated functional gene sets, central carbohydrate metabolism had the highest average
555 KEGG features per sample (13,145 ± 3,848), followed by methanogenesis (1,434 ± 423), CcO
556 (1,325 ± 398.26), and denitrification (350 ± 111).

557 The four functional gene categories (denitrification, methanogenesis, central
558 carbohydrate metabolism, and CcO) showed varying responses to plant and hydrologic treatment
559 but no response to interactions between plant and hydrologic treatments. Carbohydrate metabolic
560 composition differed between hydrologic treatments (PERMANOVA, $F_{1, 23} = 2.735$, $R^2 = 0.092$,
561 $p = 0.013$). In contrast, the compositions of denitrification genes, methanogenesis genes, and
562 CcO genes were similar across hydrologic treatments (Appendix S1: Table S6). Plant
563 presence/absence had no significant impact on the composition of functional genes (Appendix
564 S1: Table S6). Hydrologic history influenced the composition of genes associated with
565 methanogenesis, central carbohydrate metabolism, and CcO (Appendix S1: Table S6).

566 Based on environmental fitting (*vegan::envfit*), denitrification functional gene
567 composition correlated with carbon losses via CO_2 flux. Specifically, CO_2 fluxes correlated with
568 the PCoA ordination of functional gene composition associated with denitrification (envfit, R^2 =
569 0.243, $p = 0.063$, Figure 6). The compositions of functional genes involved in methanogenesis
570 and central carbohydrate metabolism were not strongly correlated with GHG fluxes but were
571 significantly ($p < 0.1$) impacted by soil redox conditions. The PCoA of methanogenesis genes
572 correlated with percent soil moisture (envfit, $R^2 = 0.201$, $p = 0.094$), and the PCoA of central
573 carbohydrate metabolism genes correlated with the percent of paint removed from IRIS tubes
574 (envfit, $R^2 = 0.238$, $p = 0.059$, Figure 6). The composition of CcO genes did not vary
575 significantly with either GHG fluxes or soil redox conditions (Figure 6).
576

Relationships between GHG fluxes, microbial community composition, and soil properties

Microbial community composition explained more of the variance in GHG fluxes than did soil properties. The DBPLSR analysis revealed that microbial community composition explained 58%, 37%, and 47% (components 1 and 2) of the variance in concentrations of CH_4, CO_2, and N_2O fluxes, respectively (Appendix S1: Table S10). Patterns in soil properties, on the other hand, only explained 19%, 29%, and 26% of the variance in concentrations of CH_4, CO_2, and N_2O fluxes, respectively, based on components 1 and 2 (Appendix S1: Table S10).

We evaluated relationships among the variance in GHG fluxes and functional gene composition at the beginning ('start') and end of the experiment ('final') using DBPLSR. Denitrification gene composition explained 54% of the variance in N_2O production at the start of the experiment, and 60% of the variance in N_2O fluxes at the end of the experiment (Appendix S1: Table S10, components 1 and 2). Methanogenesis functional gene composition explained a higher proportion of variance in CH_4 fluxes in 'start' samples (63%) than 'final' samples (33%) (Appendix S1: Table S10, components 1 and 2). 'Start' compositions of CcO and carbohydrate metabolism explained 91% and 98% of variance in CO_2 fluxes, respectively (Appendix S1: Table S10, components 1 and 2). At the end of the experiment, CcO composition only accounted for -0.67% of the variance in CO_2 fluxes, while carbohydrate metabolism explained 40% of the variance in CO_2 fluxes (Appendix S1: Table S10, components 1 and 2).

Discussion

The presence of plants and dynamic hydrology interact to affect microbial community structure and function. This study revealed that initial hydrologic conditions, compared to manipulated hydrology, strongly influenced microbial community and functional composition.

Specifically, results showed that hydrology is a strong environmental filter that determines microbial taxonomic and functional community patterns, short-term redox changes that are most distinct from historic redox conditions shift microbial communities, and plant presence can mitigate flood-induced reducing conditions and mediate greenhouse gas production.

Plant presence and dynamic hydrology influence greenhouse gas production to different degrees

Plant and hydrologic treatment strongly affected microbial function, despite hydrologic history acting as a robust environmental filter on microbial community composition. Plants can influence GHG fluxes by consuming CO_2 during photosynthesis, releasing CO_2 during respiration, aerating soils in contact with roots, and releasing labile C from roots, which can stimulate microbial activity (Luan and Wu 2014; Chanton 2005; Carmichael et al. 2014).

In the current study, soil redox status as visualized with IRIS tubes indicated that oxidizing conditions existed near plant roots (Appendix S1: Figure S1). This result suggests that plants can transport oxygen below ground. Regardless of hydrologic history, CH_4 fluxes were highest, and CO_2 fluxes were lowest in soils experiencing the wet hydrologic treatment (Figure 4). Differences in CH_4 and CO_2 fluxes were commonly observed between the dry and wet treatments (Figure 4). GHG fluxes in the interim treatment occasionally varied from those in the dry and/or wet treatments (Figure 4). Plant presence or absence also impacted GHG fluxes, especially CO_2 (Figure 3). O_2 radiation from plant roots could decrease soil CH_4 flux by providing methanotrophs with needed O_2 for CH_4 consumption, thereby decreasing CH_4 emissions in the presence of plants (Chanton 2005; Truu, Juhanson, and Truu 2009). However, counts of methanotrophic functional genes were low across samples and were unresponsive to the presence or absence of plants (Finlay and Peralta 2025). Alternatively, methanogens may be

623 inhibited or outcompeted in the presence of O_2 (Bethke et al. 2011; Cedervall et al. 2010), like
624 the conditions found near plant roots. In this study, random effects (sample mesocosm and date)
625 predominantly explained CH_4 fluxes, with a small amount of variance attributed to plant
626 presence/absence (Appendix S1: Table S4).

627 The decline in CO_2 fluxes in the presence of plants could be due to plant photosynthesis
628 and plant uptake of atmospheric CO_2 from within the collection chamber (Luan and Wu 2014).
629 This study provides evidence that plants decrease total CO_2 fluxes via photosynthesis, while
630 hydrologic conditions (dry vs. wet) dictate soil CO_2 and CH_4 fluxes. Plants consistently
631 decreased CO_2 fluxes throughout the experiment, while differences in GHG fluxes between
632 hydrologic treatments were more variable. Therefore, models of wetland GHG emissions should
633 consider plant cover as a stable control of CO_2 fluxes. Conversely, the impacts of soil moisture
634 on GHG fluxes vary dynamically over time and may require finer temporal resolution soil
635 moisture measurements to model GHG fluxes accurately.

636

637 *Past hydrology predicts bacterial community composition of key functional taxa*

638 For this study, we collected wetland mesocosm soils from wet, dry, and interim
639 hydrologic histories from a restored wetland. These differences in hydrologic history resulted in
640 different microbial community patterns, with wet hydrology being the most distinct compared to
641 microbial communities from the dry and interim hydrology. Specifically, dry hydrologic
642 histories were represented by taxa in the genus *Gaiella*, which are classified as strict aerobes
643 (Albuquerque et al. 2011). Wet hydrologic histories were uniquely identified by bacterial and
644 archaeal taxa putatively associated with methanogenesis, methanotrophy, and iron reduction.
645 These microbial processes occur in low-redox, low-O_2 systems (Burgin et al. 2011). Microbes

646 that are facultative anaerobes can shift between aerobic and anaerobic respiration based on soil
647 redox conditions; therefore, they can metabolically shift during dynamic soil hydrologic
648 conditions. However, obligate anaerobes, such as methanogens, are sensitive to soil oxygen
649 concentrations and desiccation (Fetzer, Bak, and Conrad 1993). For example, in a study of peat
650 bog layers, oxic subsurface layers contained more methanotrophs than methanogens, which were
651 found only in anoxic layers near the bottom of the bog (Lew and Glińska-Lewczuk 2018). This
652 suggests that hydrology is a strong determinant of O_2 availability in soils and that wet hydrologic
653 histories best support microbial communities involved in anaerobic processes.
654
655 *Mismatch between bacterial community composition and GHG function*
656 The DNA-based functional gene composition explained more variance in GHG fluxes
657 measured at the beginning of the experiment than at the end of the experiment. Hydrologic
658 history influenced wetland soil microbial community composition more than contemporary
659 treatments, which was emphasized in these results. The decrease in the strength of structure-
660 function associations from the beginning to the end of the experiment could be due to the DNA-
661 based molecular measurement providing insight into historical and integrated environmental
662 conditions, rather than contemporary changes to redox conditions. For example, DNA from
663 dormant and dead cells contributes to DNA-based community composition, and these relic
664 signatures are more indicative of past than present conditions (Lennon et al. 2018). Changes to
665 functional gene composition over the eight-week experiment may have been obscured by the
666 stable pool of dormant and relic DNA, thereby weakening structure-function relationships, as
667 observed here for CH_4 ~ methanogenesis, CO_2 ~ central carbohydrate metabolism, and CO_2 ~
668 CcO (Appendix S1: Table S10).

669 Another explanation for the decreased structure-function associations could be the
670 differences in temporal resolution between DNA-based molecular methods and *in situ* GHG
671 measurements. Differential gene expression can substantially alter CH_4 yields (Shi et al. 2014),
672 and protein expression and activity of various pathways may be altered in response to O_2
673 concentrations (e.g., (Lynch and Lin 1996) reviewed in (Saleh-Lakha et al. 2005)). These
674 changes to gene expression and protein activity could alter GHG production rapidly, while
675 changes to DNA abundance could alter GHG production over multiple microbial generations.
676 Mesocosm microbial communities in the present study likely responded to experimental
677 treatments (hydrology and plant presence or absence) by altering gene expression and protein
678 activity and shifting the abundance of functional genes over generations. Those slower changes
679 to functional gene abundance were likely difficult to detect after eight weeks using DNA-based
680 methods, hence the weakening of structure-function relationships in CH_4 and CO_2 production at
681 the end of the experiment.
682
683 *Functional gene composition predicts greenhouse gas fluxes to varying degrees*
684 *Cytochrome C oxidase*
685 To further examine microbial functional composition and GHG fluxes, we subset the
686 metagenomic data to focus on the composition of prokaryotic CcO genes as an indicator of
687 aerobic respiration in oxidizing conditions. While hydrologic history significantly influenced
688 CcO composition, CcO composition did not explain significant variance in GHG fluxes during
689 the eight-week incubation (Figure 6, Appendix S1: Table S6, Table S10). This lack of
690 explanatory power is unsurprising, given the diversity of O_2-reducing terminal oxidases and the
691 known presence of CcO genes in strict anaerobes (Esposti 2020; Jabłońska and Tawfik 2019).

692 There is no single enzyme that can be used to distinguish between aerobic and anaerobic
693 phenotypes because aerobic and anaerobic organisms do not exist as binary groups (Jabłońska
694 and Tawfik 2019). Instead, a spectrum of oxygen usage phenotypes exists (Jabłońska and Tawfik
695 2019). Evaluating the presence and number of a full suite of O_2-utilizing enzymes may be a
696 useful indicator of aerobic vs. anaerobic status (Jabłońska and Tawfik 2019). Therefore,
697 bioinformatic methods to facilitate this method ought to be further developed.
698
699 *Central carbohydrate metabolism*
700 While CcO composition was unable to explain differences in CO_2 production across
701 treatments, the composition of central carbohydrate metabolism genes was strongly related to
702 differences in hydrologic history, hydrologic treatment, and the production of CO_2 (Figure 6,
703 Appendix S1: Table S6, Table S10). In a past study, results revealed a significant positive
704 correlation between carbohydrate-active enzyme abundance and cumulative respiration in a
705 tundra soil warming experiment (Johnston et al. 2019). Similarly, carbohydrate metabolism
706 genes predicted differences in soil respiration between paddy and upland soils (Liu et al. 2020).
707 While Johnston et al. also found a relationship between CcO relative abundance and reducing
708 conditions, this was the only study we could find that successfully used CcO genes as an
709 indicator of redox conditions. Johnston et al. also found the total relative abundance of
710 carbohydrate-active enzyme genes to be significantly positively related to cumulative ecosystem
711 respiration (Johnston et al. 2019). The Liu et al. study identified several carbohydrate
712 metabolism genes as significant predictors of respiration rates in upland versus paddy soils (Liu
713 et al. 2020). While there is no single gene or defined collection of genes that have been
714 consistently used to explain microbial community respiration responses to redox changes,

715 various collections of carbohydrate metabolism genes may reflect differences in soil redox status
716 and respiration (Johnston et al. 2019; Liu et al. 2020).
717
718 *Denitrification*
719 When examining denitrifier community composition and GHG production, results
720 showed that the composition of denitrification functional genes correlated with CO_2
721 concentrations but not N_2O concentrations (Figure 6). The lack of association with N_2O is
722 unsurprising since the denitrifier community composition included the suite of genes involved in
723 the reduction of NO_3^- to N_2, with N_2O as an intermediate product that could be consumed before
724 detection via gas chromatography. The association between denitrification and CO_2 production is
725 likely the result of heterotrophic denitrification, where organic matter is oxidized to CO_2 with
726 NO_3^- as an electron acceptor (Dlamini et al. 2020). Heterotrophic denitrification, a form of
727 respiratory denitrification, is typically a facultative process, found in organisms with the ability
728 to respire aerobically when O_2 is available, and also use NO_3^- to respire anaerobically when O_2
729 availability decreases (Tiedje, Simkins, and Groffman 1989). A denitrification community-level
730 response to soil hydrologic history and experimental drying/wetting has also been observed in a
731 previous incubation experiment (Peralta, Ludmer, and Kent 2013).
732
733 *Methanogenesis*
734 In the present study, we observed that hydrologic history, rather than contemporary
735 hydrologic treatment, influenced the methanogenesis functional gene composition (Figure 6,
736 Appendix S1: Table S6). Methanogenesis has historically been described as a specialized
737 metabolism, in which methanogens are obligate anaerobes and obligate methanogens (meaning

738 they do not use alternative electron acceptors to grow) (Lyu et al. 2018). While atypical methane
739 synthesis pathways have recently been discovered (e.g., aerobic bacterial methane synthesis)
740 (Wang et al. 2021), classical anaerobic methanogenesis is still recognized as the primary source
741 of biogenic methane production (Lyu et al. 2018). In the present study, our results showed a
742 strong influence of hydrologic history on methanogen functional gene composition, which
743 supports the classical view of methanogenesis: a specialized and strictly anaerobic metabolism
744 was maintained in the historically wet (i.e., low O_2) field conditions, and this history dictated
745 mesocosms' methane production capacity. The structure-function analysis (based on DBPLSR)
746 provides another line of evidence that hydrologic history influenced methane production, where
747 methanogen functional gene composition explained a greater proportion of variance in CH_4
748 production at the start of the experiment than at the end of the experiment (Appendix S1: Table
749 S10).
750
751 *Considering plant-microbe relationships is critical to estimating wetland carbon storage*
752 *potential*
753 Our work highlights the importance of considering plant contributions to GHG emissions.
754 Many studies investigating GHG emissions use opaque chambers to decrease heating of the
755 headspace; however, these chambers can bias measurements of CH_4 emissions (Günther et al.
756 2014; Luan and Wu 2014). In most cases, plant inclusion and plant species considerations would
757 decrease the total estimation of CH_4 emissions from wetlands (Günther et al. 2014; Luan and Wu
758 2014). We found a small effect of plant presence on CH_4 fluxes, but a significant and consistent
759 decrease in CO_2 fluxes in the presence of plants. These findings suggest that to improve

estimations of C storage in wetlands, plant presence and hydrologic status should be considered to understand wetlands' potential to be a C sink.

Further, increasing extreme weather events cause changes in the duration of drought or excessive rainfall, which will alter microbial ecosystem functions (Jansson and Hofmockel 2020). Changes in precipitation regimes could directly alter soil hydrology or plant community composition (Jansson and Hofmockel 2020). Results from this study revealed that the longer the duration of hydrologic change, the more dramatic the change in ecosystem functions. These results can be used to infer what might happen during an extreme drought event. One potential scenario is that during early summer, a saturated non-tidal coastal plain wetland experiences decreased rainfall to the degree that the first meter of soil completely dries out and kills all vegetation. This may temporarily decrease CH_4 emissions, but if the same area becomes saturated again in the following month, CH_4 and CO_2 emissions could increase due to the lack of vegetation. However, if the duration of drying alters the microbial community structure, then CH_4 production may be decreased upon re-flooding since obligate anaerobes will be less persistent under drier, more aerated conditions (Angel, Claus, and Conrad 2012). This warrants future studies to more closely examine the temporal component of hydrologic changes that permanently alter microbial community structure and lead to unexpected changes to ecosystem functions.

Acknowledgments

We thank J. LeCrone, L. Armstrong, M. Stillwagon, G. Gunderson, C. Eakins, J. Basco, and C. Bledsoe for field and laboratory assistance. We thank J. Gill and the East Carolina University grounds crew for their efforts in maintaining the grounds surrounding the shade

house. We also thank M. Muscarella for contributions to microbiome analyses and anonymous reviewers for feedback on earlier versions of this manuscript. This work was supported by the National Science Foundation (Graduate Research Fellowship Program [GRFP] grant to R.B.B. and grant DEB #1845845 and CNH2 #2009185 to A.L.P.). This material is based upon work supported by the National Science Foundation under grant no. DGE-2125684. Any opinions, findings, and conclusions or recommendations expressed in this material are those of the author(s) and do not necessarily reflect the views of the National Science Foundation. The metagenomes were produced by the DOE JGI under the Community Science Program (CSP) (JGI CSP grant 503952). The work conducted by the DOE JGI, a DOE Office of Science User Facility, is supported under contract DE-AC02-05CH11231.

Conflict of Interest Statement

The authors report no conflicts of interest.

References

Albuquerque, Luciana, Luís França, Fred A. Rainey, Peter Schumann, M. Fernanda Nobre, and Milton S. Da Costa. 2011. "Gaiella Occulta Gen. Nov., Sp. Nov., a Novel Representative of a Deep Branching Phylogenetic Lineage within the Class Actinobacteria and Proposal of Gaiellaceae Fam. Nov. and Gaiellales Ord. Nov." *Systematic and Applied Microbiology* 34 (8): 595–99. https://doi.org/10.1016/j.syapm.2011.07.001.

Alldred, Mary, and Stephen B. Baines. 2016. "Effects of Wetland Plants on Denitrification Rates: A Meta-Analysis." *Ecological Applications* 26 (3): 676–85. https://doi.org/10.1890/14-1525.

Angel, Roey, Peter Claus, and Ralf Conrad. 2012. "Methanogenic Archaea Are Globally Ubiquitous in Aerated Soils and Become Active under Wet Anoxic Conditions." *The ISME Journal* 6 (4): 847–62. https://doi.org/10.1038/ismej.2011.141.

Apprill, Amy, Sean Mcnally, Rachel Parsons, and Laura Weber. 2015. "Minor Revision to V4 Region SSU rRNA 806R Gene Primer Greatly Increases Detection of SAR11 Bacterioplankton." *Aquatic Microbial Ecology* 75 (2): 129–37. https://doi.org/10.3354/ame01753.

Ardón, Marcelo, Jennifer L. Morse, Benjamin P. Colman, and Emily S. Bernhardt. 2013. "Drought-Induced Saltwater Incursion Leads to Increased Wetland Nitrogen Export." *Global Change Biology* 19 (10): 2976–85. https://doi.org/10.1111/gcb.12287.

Ardón, Marcelo, Jennifer L. Morse, Martin W. Doyle, and Emily S. Bernhardt. 2010. "The Water Quality Consequences of Restoring Wetland Hydrology to a Large Agricultural Watershed in the Southeastern Coastal Plain." *Ecosystems* 13 (7): 1060–78. https://doi.org/10.1007/s10021-010-9374-x.

Bartoń, Kamil. 2025. “MuMIn: Multi-Model Inference.” https://cran.r-project.org/web/packages/MuMIn/index.html.

Bates, D, M Machler, B Bolker, and S Walker. 2015. “Fitting Linear Mixed-Effects Models Using Lme4.” *Journal of Statistical Software* 67 (1): 1–48. https://doi.org/10.18637/jss.v067.i01.

Bethke, Craig M., Robert A. Sanford, Matthew F. Kirk, Qusheng Jin, and Theodore M. Flynn. 2011. “The Thermodynamic Ladder in Geomicrobiology.” *American Journal of Science* 311 (3): 183–210. https://doi.org/10.2475/03.2011.01.

Blanca, María J., Rafael Alarcón, Jaume Arnau, Roser Bono, and Rebecca Bendayan. 2017. “Non-Normal Data: Is ANOVA Still a Valid Option?” *Psicothema* 29 (4): 552–57. https://doi.org/10.7334/psicothema2016.383.

Boj, Eva, Adria Caballe, Pedro Delicado, and Josep Fortiana. 2024. “Dbstats: Distance-Based Statistics Version 2.0.2 from CRAN.” https://CRAN.R-project.org/package=dbstats.

Burgin, Amy J, Wendy H Yang, Stephen K Hamilton, and Whendee L Silver. 2011. “Beyond Carbon and Nitrogen: How the Microbial Energy Economy Couples Elemental Cycles in Diverse Ecosystems.” *Frontiers in Ecology and the Environment* 9 (1): 44–52. https://doi.org/10.1890/090227.

Caporaso, J Gregory, Christian L Lauber, William a Walters, Donna Berg-Lyons, James Huntley, Noah Fierer, Sarah M Owens, et al. 2012. “Ultra-High-Throughput Microbial Community Analysis on the Illumina HiSeq and MiSeq Platforms.” *The ISME Journal* 6 (8): 1621–24. https://doi.org/10.1038/ismej.2012.8.

Carmichael, M. J., E. S. Bernhardt, S. L. Bräuer, and W. K. Smith. 2014. “The Role of Vegetation in Methane Flux to the Atmosphere: Should Vegetation Be Included as a

Distinct Category in the Global Methane Budget?" *Biogeochemistry* 119 (1–3): 1–24. https://doi.org/10.1007/s10533-014-9974-1.

Cedervall, Peder E., Mishtu Dey, Arwen R. Pearson, Stephen W. Ragsdale, and Carrie M. Wilmot. 2010. "Structural Insight into Methyl-Coenzyme M Reductase Chemistry Using Coenzyme B Analogues,." *Biochemistry* 49 (35): 7683–93. https://doi.org/10.1021/bi100458d.

Chanton, Jeffrey P. 2005. "The Effect of Gas Transport on the Isotope Signature of Methane in Wetlands." *Organic Geochemistry* 36 (5): 753–68. https://doi.org/10.1016/j.orggeochem.2004.10.007.

Chen, I-Min A., Victor M. Markowitz, Ken Chu, Krishna Palaniappan, Ernest Szeto, Manoj Pillay, Anna Ratner, et al. 2017. "IMG/M: Integrated Genome and Metagenome Comparative Data Analysis System." *Nucleic Acids Research* 45 (D1): D507–16. https://doi.org/10.1093/nar/gkw929.

Conrad, Ralf. 2009. "The Global Methane Cycle: Recent Advances in Understanding the Microbial Processes Involved." *Environmental Microbiology Reports* 1 (5): 285–92. https://doi.org/10.1111/j.1758-2229.2009.00038.x.

Dlamini, J. C., D. Chadwick, J. M. B. Hawkins, J. Martinez, D. Scholefield, Y. Ma, and L. M. Cárdenas. 2020. "Evaluating the Potential of Different Carbon Sources to Promote Denitrification." *The Journal of Agricultural Science* 158 (3): 194–205. https://doi.org/10.1017/S0021859620000520.

Esposti, Mauro Degli. 2020. "On the Evolution of Cytochrome Oxidases Consuming Oxygen." *Biochimica et Biophysica Acta (BBA) - Bioenergetics* 1861 (12): 148304. https://doi.org/10.1016/j.bbabio.2020.148304.

Fetzer, Silke, Friedhelm Bak, and Ralf Conrad. 1993. "Sensitivity of Methanogenic Bacteria from Paddy Soil to Oxygen and Desiccation." *FEMS Microbiology Ecology* 12 (2): 107–15. https://doi.org/10.1111/j.1574-6941.1993.tb00022.x.

Finlay, Colin G., and Ariane L. Peralta. 2025. "Hydrologic History and Flooding Pulses Control Iron and Sulfur Metabolic Composition with Variable Associations to Greenhouse Gas Production in a Coastal Wetland Mesocosm Experiment." bioRxiv. https://doi.org/10.1101/2025.03.03.641170.

Fluet-Chouinard, Etienne, Benjamin D. Stocker, Zhen Zhang, Avni Malhotra, Joe R. Melton, Benjamin Poulter, Jed O. Kaplan, et al. 2023. "Extensive Global Wetland Loss over the Past Three Centuries." *Nature* 614 (7947): 281–86. https://doi.org/10.1038/s41586-022-05572-6.

Fuss, Roland, and Roman Hueppi. 2024. "Gasfluxes: Greenhouse Gas Flux Calculation from Chamber Measurements." https://cran.r-project.org/web/packages/gasfluxes/index.html.

Glassman, Sydney I., and Jennifer B. H. Martiny. 2018. "Broadscale Ecological Patterns Are Robust to Use of Exact Sequence Variants versus Operational Taxonomic Units." *mSphere* 3 (4): e00148-18. https://doi.org/10.1128/mSphere.00148-18.

Gorsky, A. L., G. A. Racanelli, A. C. Belvin, and R. M. Chambers. 2019. "Greenhouse Gas Flux from Stormwater Ponds in Southeastern Virginia (USA)." *Anthropocene* 28. https://doi.org/10.1016/j.ancene.2019.100218.

Günther, Anke, Gerald Jurasinski, Vytas Huth, and Stephan Glatzel. 2014. "Opaque Closed Chambers Underestimate Methane Fluxes of Phragmites Australis (Cav.) Trin. Ex Steud." *Environmental Monitoring and Assessment* 186 (4): 2151–58. https://doi.org/10.1007/s10661-013-3524-5.

Havlicek, Larry L., and Nancy L. Peterson. 1974. "Robustness of the T Test: A Guide for Researchers on Effect of Violations of Assumptions." *Psychological Reports* 34 (3_suppl): 1095–1114. https://doi.org/10.2466/pr0.1974.34.3c.1095.

Hoffmann, Mathias, Natalia Pehle, Vytas Huth, Nicole Jurisch, Michael Sommer, and Jürgen Augustin. 2018. "A Simple Method to Assess the Impact of Sealing, Headspace Mixing and Pressure Vent on Airtightness of Manually Closed Chambers." *Journal of Plant Nutrition and Soil Science* 181 (1): 36–40. https://doi.org/10.1002/jpln.201600299.

Hopfensperger, Kristine N., Amy J. Burgin, Valerie A. Schoepfer, and Ashley M. Helton. 2014. "Impacts of Saltwater Incursion on Plant Communities, Anaerobic Microbial Metabolism, and Resulting Relationships in a Restored Freshwater Wetland." *Ecosystems* 17 (5): 792–807. https://doi.org/10.1007/s10021-014-9760-x.

Hu, Qiwu, Jiayan Cai, Bo Yao, Qin Wu, Yeqiao Wang, and Xingliang Xu. 2015. "Plant-Mediated Methane and Nitrous Oxide Fluxes from a Carex Meadow in Poyang Lake during Drawdown Periods." *Plant and Soil*. https://doi.org/10.1007/s11104-015-2733-9.

Huntemann, Marcel, Natalia N. Ivanova, Konstantinos Mavromatis, H. James Tripp, David Paez-Espino, Kristin Tennessen, Krishnaveni Palaniappan, et al. 2016. "The Standard Operating Procedure of the DOE-JGI Metagenome Annotation Pipeline (MAP v.4)." *Standards in Genomic Sciences* 11 (1): 17. https://doi.org/10.1186/s40793-016-0138-x.

Hurvich, C, and C Tsai. 1993. "A CORRECTED AKAIKE INFORMATIONON CRITERION FOR VECTOR AUTOREGRESSIVE MODEL SELECTION." *Journal of Time Series Analysis* 14 (3): 271–79.

Jabłońska, Jagoda, and Dan S. Tawfik. 2019. "The Number and Type of Oxygen-Utilizing Enzymes Indicates Aerobic vs. Anaerobic Phenotype." *Free Radical Biology and*

Medicine, Early Life on Earth and Oxidative Stress, 140 (August):84–92. https://doi.org/10.1016/j.freeradbiomed.2019.03.031.

Jansson, Janet K., and Kirsten S. Hofmockel. 2020. "Soil Microbiomes and Climate Change." *Nature Reviews Microbiology* 18 (1): 35–46. https://doi.org/10.1038/s41579-019-0265-7.

Jenkinson, B. J., and D. P. Franzmeier. 2006. "Development and Evaluation of Iron-Coated Tubes That Indicate Reduction in Soils." *Soil Science Society of America Journal* 70 (1): 183–91. https://doi.org/10.2136/sssaj2004.0323.

Johnston, Eric R., Janet K. Hatt, Zhili He, Liyou Wu, Xue Guo, Yiqi Luo, Edward A. G. Schuur, James M. Tiedje, Jizhong Zhou, and Konstantinos T. Konstantinidis. 2019. "Responses of Tundra Soil Microbial Communities to Half a Decade of Experimental Warming at Two Critical Depths." *Proceedings of the National Academy of Sciences* 116 (30): 15096–105. https://doi.org/10.1073/pnas.1901307116.

Kim, Seon Young, Seung Hoon Lee, Chris Freeman, Nathalie Fenner, and Hojeong Kang. 2008. "Comparative Analysis of Soil Microbial Communities and Their Responses to the Short-Term Drought in Bog, Fen, and Riparian Wetlands." *Soil Biology and Biochemistry* 40 (11): 2874–80. https://doi.org/10.1016/j.soilbio.2008.08.004.

Kimball, Spencer, Peter Mattis, Michael Natterer, and Jehan. 2014. "GIMP." https://www.gimp.org/.

Kingsford, Richard T., Alberto Basset, and Leland Jackson. 2016. "Wetlands: Conservation's Poor Cousins." *Aquatic Conservation: Marine and Freshwater Ecosystems* 26 (5): 892–916. https://doi.org/10.1002/aqc.2709.

Kozich, James J., Sarah L. Westcott, Nielson T. Baxter, Sarah K. Highlander, and Patrick D. Schloss. 2013. "Development of a Dual-Index Sequencing Strategy and Curation Pipeline

for Analyzing Amplicon Sequence Data on the Miseq Illumina Sequencing Platform." *Applied and Environmental Microbiology* 79 (17): 5112–20. https://doi.org/10.1128/AEM.01043-13.

Kuzyakov, Yakov. 2010. "Soil Biology & Biochemistry Priming Effects : Interactions between Living and Dead Organic Matter." *Soil Biology and Biochemistry* 42 (9): 1363–71. https://doi.org/10.1016/j.soilbio.2010.04.003.

Lennon, J. T., M. E. Muscarella, S. A. Placella, and B. K. Lehmkuhl. 2018. "How, When, and Where Relic DNA Affects Microbial Diversity." *mBio* 9 (3): 10.1128/mbio.00637-18. https://doi.org/10.1128/mbio.00637-18.

Lennon, Jay T., and Stuart E. Jones. 2011. "Microbial Seed Banks: The Ecological and Evolutionary Implications of Dormancy." *Nature Reviews Microbiology* 9 (2): 119–30. https://doi.org/10.1038/nrmicro2504.

Lew, Sylwia, and Katarzyna Glińska-Lewczuk. 2018. "Environmental Controls on the Abundance of Methanotrophs and Methanogens in Peat Bog Lakes." *Science of the Total Environment* 645:1201–11. https://doi.org/10.1016/j.scitotenv.2018.07.141.

Liu, Yu-Rong, Manuel Delgado-Baquerizo, Ziming Yang, Jiao Feng, Jun Zhu, and Qiaoyun Huang. 2020. "Microbial Taxonomic and Functional Attributes Consistently Predict Soil CO2 Emissions across Contrasting Croplands." *Science of The Total Environment* 702 (February):134885. https://doi.org/10.1016/j.scitotenv.2019.134885.

Luan, Junwei, and Jianghua Wu. 2014. "Gross Photosynthesis Explains the 'artificial Bias' of Methane Fluxes by Static Chamber (Opaque versus Transparent) at the Hummocks in a Boreal Peatland." *Environmental Research Letters* 9 (10). https://doi.org/10.1088/1748-9326/9/10/105005.

Lynch, A S, and E C Lin. 1996. “Transcriptional Control Mediated by the ArcA Two-Component Response Regulator Protein of Escherichia Coli: Characterization of DNA Binding at Target Promoters.” *Journal of Bacteriology* 178 (21): 6238–49. https://doi.org/10.1128/jb.178.21.6238-6249.1996.

Lyu, Zhe, Nana Shao, Taiwo Akinyemi, and William B. Whitman. 2018. “Methanogenesis.” *Current Biology* 28 (13): R727–32. https://doi.org/10.1016/j.cub.2018.05.021.

Markowitz, Victor M., I-Min A. Chen, Ken Chu, Ernest Szeto, Krishna Palaniappan, Manoj Pillay, Anna Ratner, et al. 2014. “IMG/M 4 Version of the Integrated Metagenome Comparative Analysis System.” *Nucleic Acids Research* 42 (D1): D568–73. https://doi.org/10.1093/nar/gkt919.

McDonald, I R, and J C Murrell. 1997. “The Methanol Dehydrogenase Structural Gene mxaF and Its Use as a Functional Gene Probe for Methanotrophs and Methylotrophs.” *FEMS Microbiology Letters* 156 (8): 205–10.

Mehlich, A. 1984. “Mehlich 3 Soil Test Extractant: A Modification of Mehlich 2 Extractant.” *Communications in Soil Science and Plant Analysis* 15 (12): 1409–16. https://doi.org/10.1080/00103628409367568.

Mentzer, Jessica L, Robert M Goodman, and Teri C Balser. 2006. “Microbial Response over Time to Hydrologic and Fertilization Treatments in a Simulated Wet Prairie.” *Plant and Soil* 284 (1–2): 85–100. https://doi.org/10.1007/s11104-006-0032-1.

Mitsch, William J., Blanca Bernal, Amanda M. Nahlik, Ülo Mander, Li Zhang, Christopher J. Anderson, Sven E. Jørgensen, and Hans Brix. 2013. “Wetlands, Carbon, and Climate Change.” *Landscape Ecology* 28 (4): 583–97. https://doi.org/10.1007/s10980-012-9758-8.

Mitsch, William J., and James G. Gosslink. 2007. *Wetlands*. 4th ed. Hoboken: John Wiley & Sons.

Morse, Jennifer L., Marcelo Ardón, and Emily S. Bernhardt. 2012. "Greenhouse Gas Fluxes in Southeastern U.S. Coastal Plain Wetlands under Contrasting Land Uses." *Ecological Applications* 22 (1): 264–80. https://doi.org/10.1890/11-0527.1.

Mylavarapu, Rao, Tom Obreza, Kelly Morgan, George Hochmuth, Vimala Nair, and Alan Wright. 2014. "Extraction of Soil Nutrients Using Mehlich-3 Reagent for Acid-Mineral Soils of Florida." *University of Florida. Institute of Food and Agricultural Science*, no. SL407, 1–7.

Nygaard, Bettina, and Rasmus Ejrnæs. 2009. "The Impact of Hydrology and Nutrients on Species Composition and Richness: Evidence from a Microcosm Experiment." *Wetlands* 29 (1): 187–95. https://doi.org/10.1672/08-13.1.

Oksanen, Jari. 2015. "Vegan : Ecological Diversity" 1 (2): 1–12. https://doi.org/10.1029/2006JF000545.

Parada, Alma E., David M. Needham, and Jed A. Fuhrman. 2016. "Every Base Matters: Assessing Small Subunit rRNA Primers for Marine Microbiomes with Mock Communities, Time Series and Global Field Samples." *Environmental Microbiology* 18 (5): 1403–14. https://doi.org/10.1111/1462-2920.13023.

Peralta, Ariane L., Regina B. Bledsoe, Mario E. Muscarella, Marcel Huntemann, Alicia Clum, Brian Foster, Bryce Foster, et al. 2020. "Metagenomes from Experimental Hydrologic Manipulation of Restored Coastal Plain Wetland Soils (Tyrell County, North Carolina)." Edited by J. Cameron Thrash. *Microbiology Resource Announcements* 9 (41). https://doi.org/10.1128/MRA.00882-20.

Peralta, Ariane L., Sarah Ludmer, and Angela D. Kent. 2013. "Hydrologic History Influences Microbial Community Composition and Nitrogen Cycling under Experimental Drying/Wetting Treatments." *Soil Biology and Biochemistry* 66 (November):29–37. https://doi.org/10.1016/j.soilbio.2013.06.019.

Peralta, Ariane L, Sarah Ludmer, Jeffrey W Matthews, and Angela D Kent. 2014. "Bacterial Community Response to Changes in Soil Redox Potential along a Moisture Gradient in Restored Wetlands." *Ecological Engineering* 73:246–53. https://doi.org/10.1016/j.ecoleng.2014.09.047.

Peralta, Ariane L., Diana Stuart, Angela D. Kent, and Jay T. Lennon. 2014. "A Social-Ecological Framework for 'Micromanaging' Microbial Services." *Frontiers in Ecology and the Environment* 12 (9): 524–31. https://doi.org/10.1890/130308.

Philippot, Laurent, Jos M. Raaijmakers, Philippe Lemanceau, and Wim H. Van Der Putten. 2013. "Going Back to the Roots: The Microbial Ecology of the Rhizosphere." *Nature Reviews Microbiology* 11 (11): 789–99. https://doi.org/10.1038/nrmicro3109.

Quast, Christian, Elmar Pruesse, Pelin Yilmaz, Jan Gerken, Timmy Schweer, Pablo Yarza, Jörg Peplies, and Frank Oliver Glöckner. 2013. "The SILVA Ribosomal RNA Gene Database Project: Improved Data Processing and Web-Based Tools." *Nucleic Acids Research* 41 (D1): 590–96. https://doi.org/10.1093/nar/gks1219.

R Core Team. 2024. "R: A Language and Environment for Statistical Computing." Vienna, Austria: R Foundation for Statistical Computing. https://www.R-project.org/.

Rabenhorst, Martin C. 2008. "Protocol for Using and Interpreting IRIS Tubes." *Soil Survey Horizons* 49 (3): 74–77.

Roberts, David W. 2023. “Labdsv: Ordination and Multivariate Analysis for Ecology.” https://cran.r-project.org/web/packages/labdsv/index.html.

Rocca, Jennifer D, Edward K Hall, Jay T Lennon, Sarah E Evans, Mark P Waldrop, James B Cotner, Diana R Nemergut, Emily B Graham, and Matthew D Wallenstein. 2015. “Relationships between Protein-Encoding Gene Abundance and Corresponding Process Are Commonly Assumed yet Rarely Observed.” *The ISME Journal* 9 (8): 1693–99. https://doi.org/10.1038/ismej.2014.252.

Rognes, Torbjørn, Tomáš Flouri, Ben Nichols, Christopher Quince, and Frédéric Mahé. 2016. “VSEARCH: A Versatile Open Source Tool for Metagenomics.” *PeerJ* 4:e2584. https://doi.org/10.7717/peerj.2584.

Saleh-Lakha, Saleema, Michelle Miller, Rachel G. Campbell, Kim Schneider, Parastu Elahimanesh, Miranda M. Hart, and Jack T. Trevors. 2005. “Microbial Gene Expression in Soil: Methods, Applications and Challenges.” *Journal of Microbiological Methods* 63 (1): 1–19. https://doi.org/10.1016/j.mimet.2005.03.007.

Schielzeth, Holger, Niels J. Dingemanse, Shinichi Nakagawa, David F. Westneat, Hassen Allegue, Céline Teplitsky, Denis Réale, Ned A. Dochtermann, László Zsolt Garamszegi, and Yimen G. Araya-Ajoy. 2020. “Robustness of Linear Mixed-Effects Models to Violations of Distributional Assumptions.” *Methods in Ecology and Evolution* 11 (9): 1141–52. https://doi.org/10.1111/2041-210X.13434.

Schloss, Patrick D. 2021. “Amplicon Sequence Variants Artificially Split Bacterial Genomes into Separate Clusters.” *mSphere* 6 (4): e00191-21. https://doi.org/10.1128/mSphere.00191-21.

1047 Schloss, Patrick D., Sarah L. Westcott, Thomas Ryabin, Justine R. Hall, Martin Hartmann, Emily
1048 B. Hollister, Ryan a. Lesniewski, et al. 2009. "Introducing Mothur: Open-Source,
1049 Platform-Independent, Community-Supported Software for Describing and Comparing
1050 Microbial Communities." *Applied and Environmental Microbiology* 75 (23): 7537–41.
1051 https://doi.org/10.1128/AEM.01541-09.
1052 Schneider, Caroline A, Wayne S Rasband, and Kevin W Eliceiri. 2012. "NIH Image to ImageJ:
1053 25 Years of Image Analysis." *Nature Methods* 9 (7): 671–75.
1054 https://doi.org/10.1038/nmeth.2089.
1055 Schneider, Grant, Eric Chicken, and Rachel Becvarik. 2023. "NSM3: Functions and Datasets to
1056 Accompany Hollander, Wolfe, and Chicken - Nonparametric Statistical Methods, Third
1057 Edition." https://cran.r-project.org/web/packages/NSM3/index.html.
1058 Shi, Weibing, Christina D. Moon, Sinead C. Leahy, Dongwan Kang, Jeff Froula, Sandra
1059 Kittelmann, Christina Fan, et al. 2014. "Methane Yield Phenotypes Linked to Differential
1060 Gene Expression in the Sheep Rumen Microbiome." *Genome Research* 24 (9): 1517–25.
1061 https://doi.org/10.1101/gr.168245.113.
1062 Sundberg, Carina, Jenny S. Jenny, Karin Tonderski, and Per Eric Lindgren. 2007. "Overland
1063 Flow Systems for Treatment of Landfill Leachates-Potential Nitrification and Structure of
1064 the Ammonia-Oxidising Bacterial Community during a Growing Season." *Soil Biology
1065 and Biochemistry* 39 (1): 127–38. https://doi.org/10.1016/j.soilbio.2006.06.016.
1066 Tiedje, James M., Stephen Simkins, and Peter M. Groffman. 1989. "Perspectives on
1067 Measurement of Denitrification in the Field Including Recommended Protocols for
1068 Acetylene-Based Methods." *Plant and Soil* 115 (2): 261–84.
1069 https://doi.org/10.1007/BF02202594.

Truu, Marika, Jaanis Juhanson, and Jaak Truu. 2009. “Microbial Biomass, Activity and Community Composition in Constructed Wetlands.” *Science of The Total Environment* 407 (13): 3958–71. https://doi.org/10.1016/j.scitotenv.2008.11.036.

Wang, Qian, Abdullah Alowaifeer, Patricia Kerner, Narayanaganesh Balasubramanian, Angela Patterson, William Christian, Angela Tarver, et al. 2021. “Aerobic Bacterial Methane Synthesis.” *Proceedings of the National Academy of Sciences* 118 (27). https://doi.org/10.1073/pnas.2019229118.

1079 **Tables**

1080 **Table 1**. Soil chemical and physical properties measured after eight weeks of hydrologic

1081 manipulation.

Treatment	Dry		Interim		Wet	
Plant	No Plant	Plant	No Plant	Plant	No Plant	Plant
Moisture (%)	39 ± 0.31	14 ± 0.03	19 ± 0.16	13 ± 0.02	29 ± 0.23	62 ± 0.07
pH	5.31 ± 0.11	5.31 ± 0.09	5.4 ± 0.16	5.35 ± 0.1	5.55 ± 0.15	5.41 ± 0.17
NH_4^+ mg L^{-1}	0.39 ± 0.07	0.27 ± 0.04	0.26 ± 0.1	0.19 ± 0.02	0.77 ± 0.76	0.39 ± 0.42
NO_3^- mg L^{-1}	0.08 ± 0.07	MDL	0.25 ± 0.38	MDL	0.01 ± 0.0005	MDL
Total C (%)	4.63 ± 0.78	4.63 ± 0.81	4.48 ± 0.32	4.37 ± 0.52	4.91 ± 0.92	4.68 ± 0.74
Total N (%)	0.22 ± 0.03	0.22 ± 0.03	0.22 ± 0.01	0.21 ± 0.03	0.24 ± 0.04	0.23 ± 0.03
P ppm	21.00 ± 4.14	20.41 ± 4.4	23.58 ± 8.87	22.83 ± 8.37	23.16 ± 5.98	23 ± 5.79
K ppm	33.66 ± 5.97	30.25 ± 10.31	39.5 ± 11.44	26.75 ± 3.04	46.16 ± 16.02	34.25 ± 10.78
Mg ppm	77.58 ± 6.46	74.66 ± 11.43	86 ± 22.33	78.66 ± 16.47	89.25 ± 16.85	79.41 ± 18.8
S ppm	15.75 ± 1.94	15.33 ± 2.29	13.25 ± 1.25	12.16 ± 0.40	11.33 ± 1.21	11.5 ± 1.00
Fe ppm	252.66 ± 14.45	243.66 ± 17.06	275.33 ± 27.07	251.16 ± 37.6	306.83 ± 22.52	280.66 ± 40.71
Mn ppm	3.91 ± 1.15	3.41 ± 0.97	4.33 ± 1.16	4.58 ± 1.31	5.83 ± 1.32	5.58 ± 2.05
Humic matter (%)	2.35 ± 0.19	2.17 ± 0.14	2.04 ± 0.29	2.28 ± 0.22	1.98 ± 0.422	1.96 ± 0.43

1082 Notes: Average (mean ± standard deviation) by hydrologic treatment and plant status are

1083 reported to show differences among groups.

1084 Abbreviations: MDL: below detection limit, ppm: parts per million.

1085

1086

1087

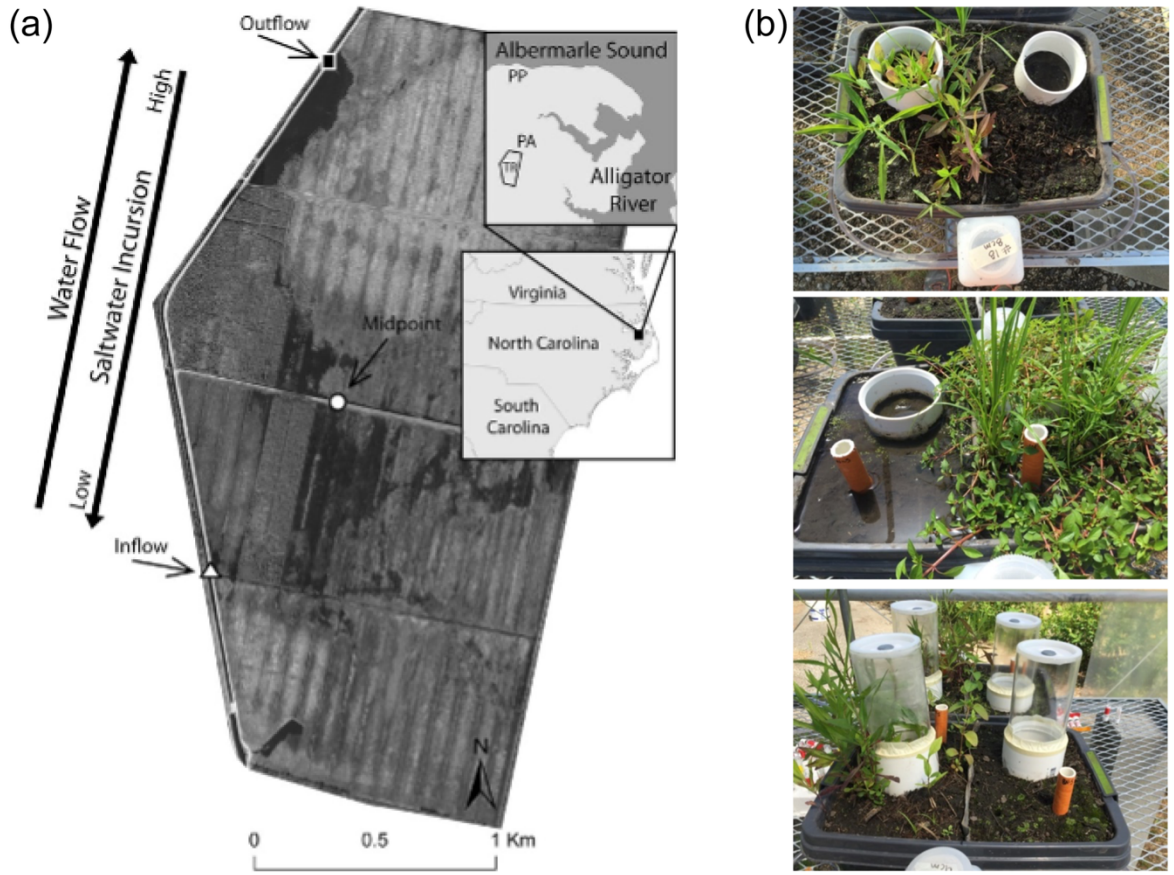

Figure 1. Field site and mesocosm set-up. Wetland mesocosms sourced from the Timberlake Observatory for Wetland Restoration (image modified with permission from Ardón et al., 2013) (a). Aerial view of wetland mesocosm setup, where the left side of the box represents plant treatment, and the right side represents no plant treatment, separated by a stainless mesh divider ((b), top, photo credit: R. Bledsoe). PVC collars installed for measuring greenhouse gas concentrations. Also shown is a 1-liter bottle attached to each side of the mesocosm used to maintain water levels. Example of a wet treatment mesocosm with IRIS tubes installed ((b), middle) (photo credit: R. Bledsoe). Example of mesocosm with prepared for GHG sampling ((b), bottom) (photo credit: R. Bledsoe).

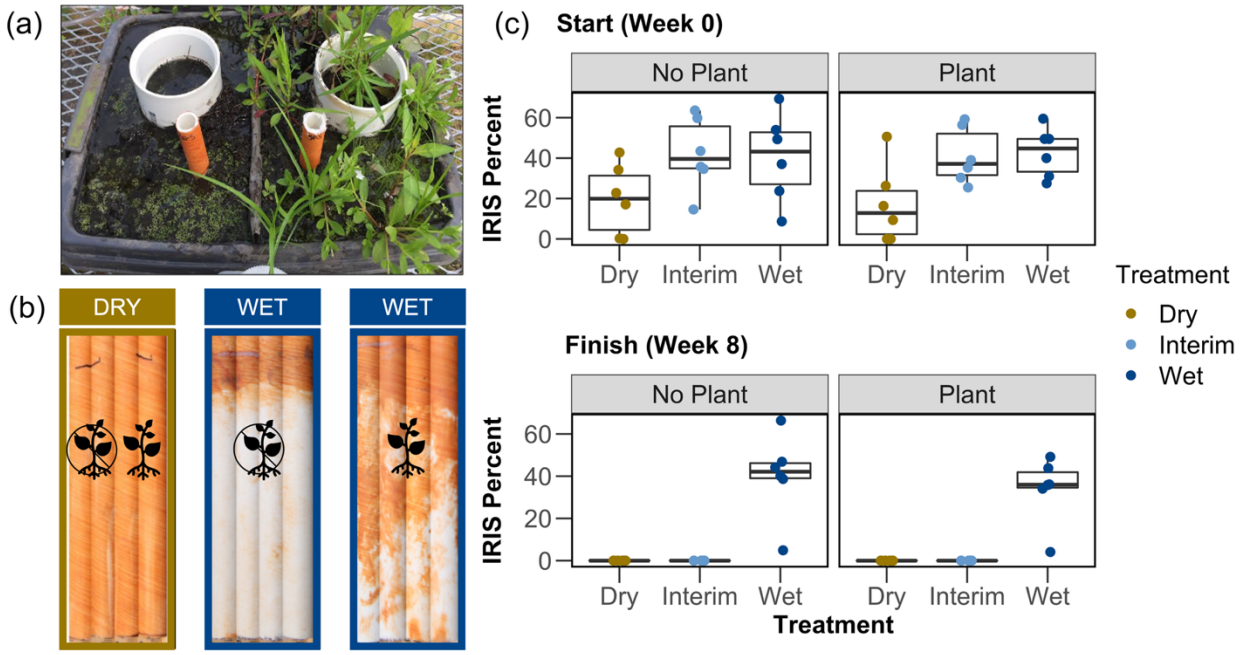

Figure 2. Indicator of reduction in soils (IRIS) tubes mesocosm image (photo credit: R. Bledsoe) (a), IRIS tube example image (photo credit: R. Bledsoe) (b), and boxplots summarizing redox status at the beginning and end of the experiment (c). Percent paint removed from IRIS tubes at the start of the experiment (week 0) and the end of the experiment (week 8). Example IRIS tubes used for ImageJ analysis post-incubation (b) with plant icons crossed out represent IRIS tubes from mesocosms with plants removed, and plant icons represent IRIS tubes from mesocosms with plants present. Box plots summarize percent paint removed from IRIS tubes at start (week 0) and finish (week 8) of experimental incubation. Color represents hydrologic treatment: brown indicates dry, light blue indicates interim, and dark blue indicates wet. Individual samples are plotted as points and colored according to their hydrologic treatment. Boxplots summarize median, first and third quartiles, and two whiskers extending |≤| 1.5 * interquartile range.

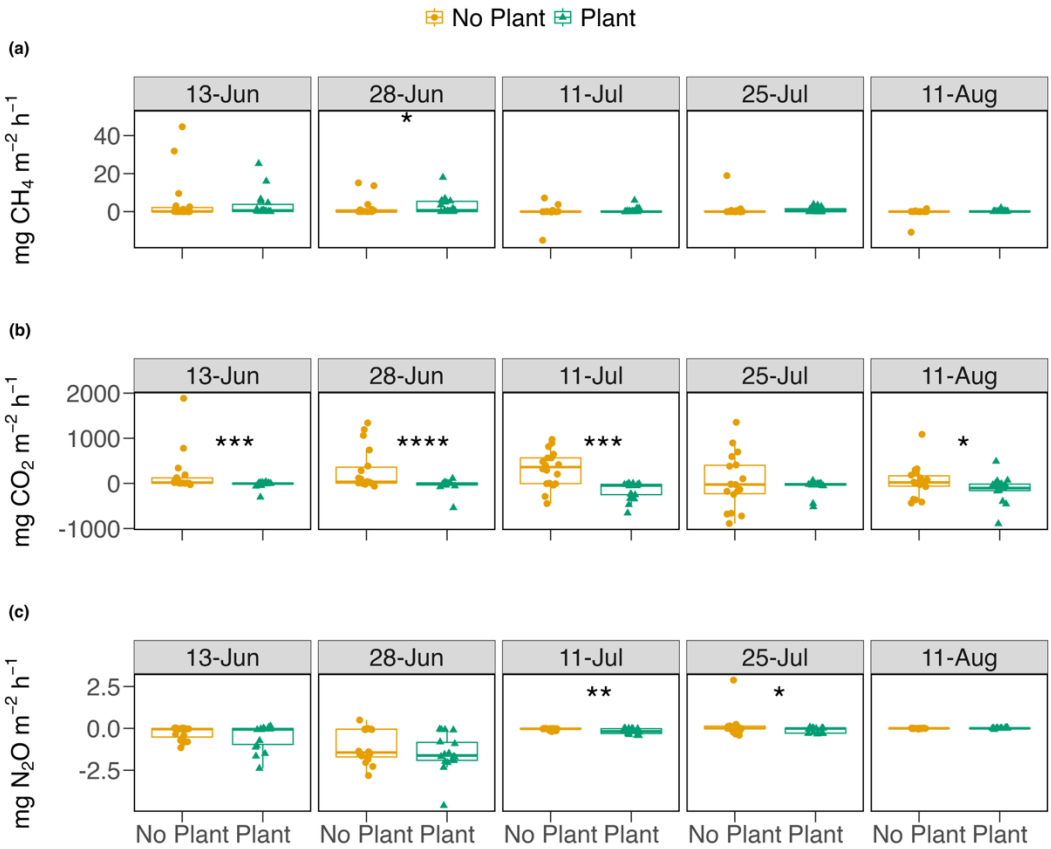

Figure 3.

Greenhouse gas fluxes comparing no plant vs. plant treatments. Fluxes are in milligrams of CH_4 (a), CO_2 (b), and N_2O (c) per square meter per hour, and are compared for plant presence/absence treatments during the five time points. Color represents plant presence/absence: orange = no plant, green = plant. Individual samples are plotted as points and colored by plant presence/absence. Boxplots summarize the median, first and third quartiles, and two whiskers extending |≤| 1.5 * interquartile range. Asterisks represent significance levels of Wilcoxon Rank-Sum tests (****: $p \leq 0.0001$, ***: $p \leq 0.001$, **: $p \leq 0.01$, *: $p \leq 0.05$, no symbol: $p > 0.05$). An extreme outlier of 248 mg CH_4 m^{-2} h^{-1}, measured in a wet treatment with no plants on July 11th, was used in statistical calculations but not displayed in the plot to improve visualization of differences across treatments.

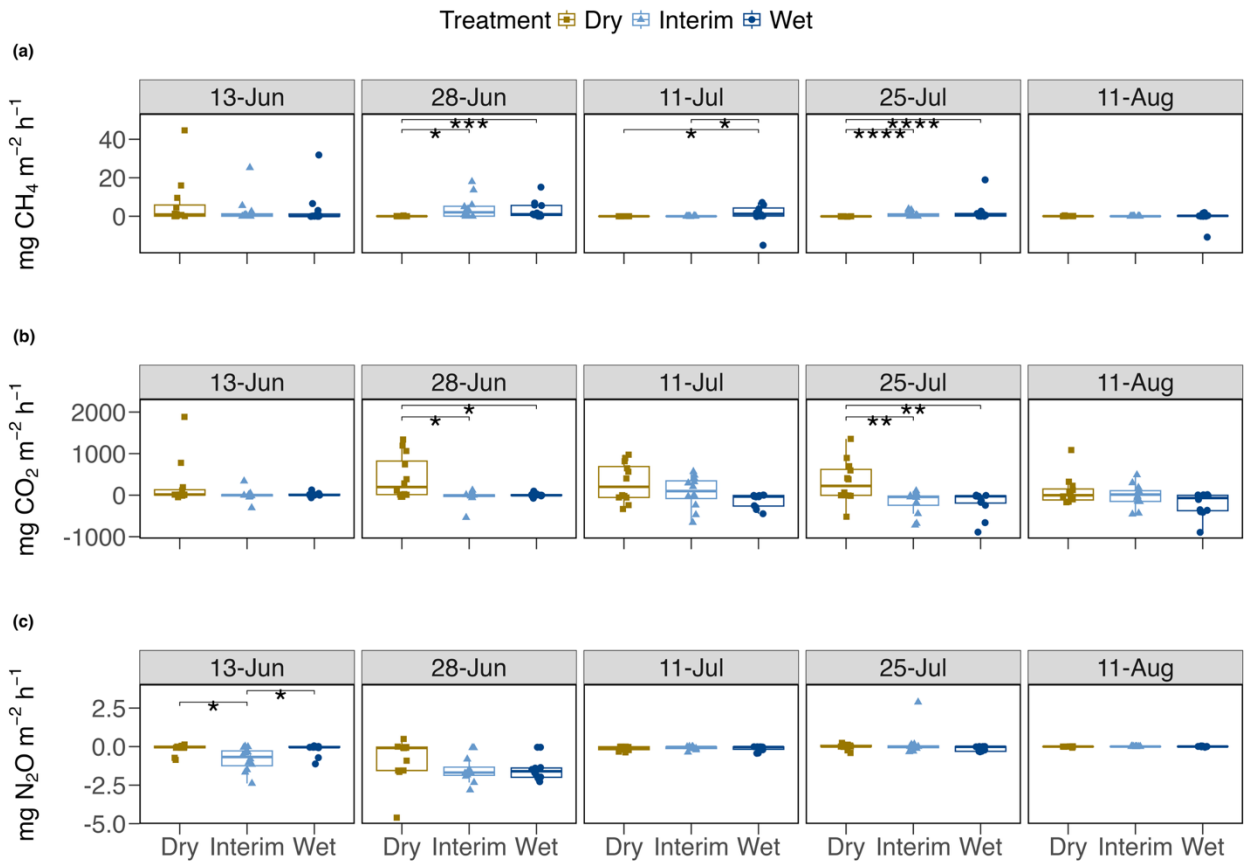

Figure 4. Greenhouse gas fluxes in dry, interim, and wet hydrologic treatments. Fluxes are in milligrams of CH_4 (a), CO_2 (b), and N_2O (c) per square meter per hour, and are compared for hydrologic treatments during the five time points. Individual samples are plotted as shapes and colored by hydrologic treatment (brown squares = dry, light blue triangles = interim, dark blue circles = wet). Boxplots summarize the median, first and third quartiles, and two whiskers extending |≤| 1.5 * interquartile range. Asterisks represent significance levels of Dwass, Steel, Critchlow, and Fligner (SDCFlig) tests (****: $p \leq 0.0001$, ***: $p \leq 0.001$, **: $p \leq 0.01$, *: $p \leq 0.05$, no symbol: $p > 0.05$). An extreme outlier of 248 mg CH_4 m^{-2} h^{-1}, measured in a wet treatment with no plants on July 11th, was used in statistical calculations but not displayed in the plot to improve visualization of differences across treatments.

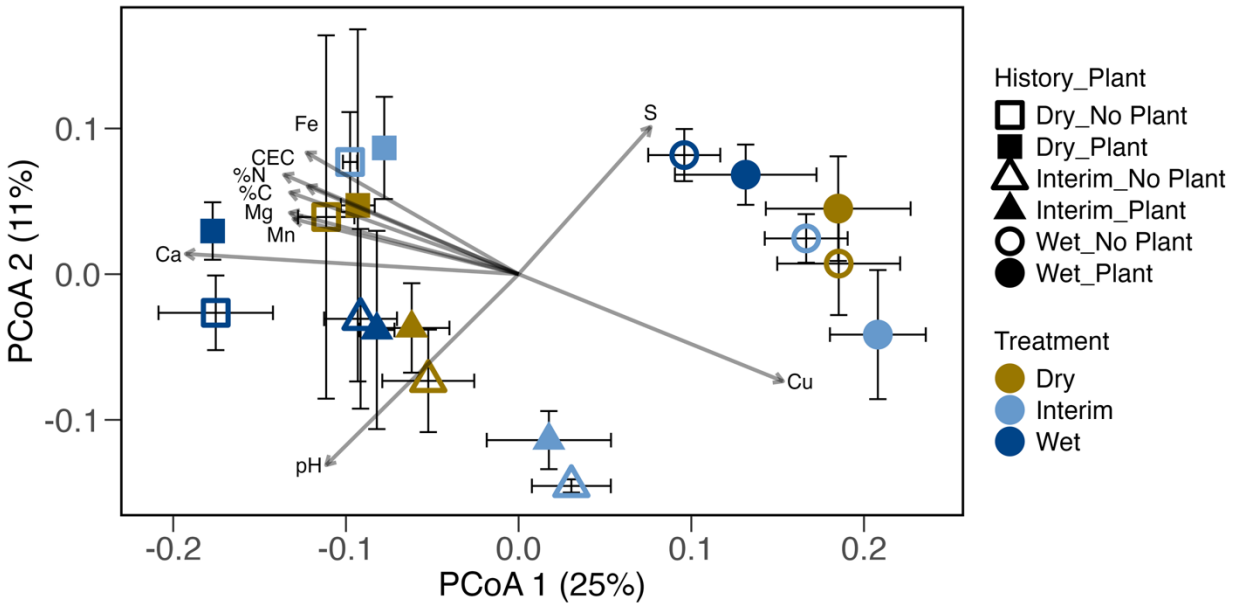

Figure 5. Ordination based on a principal coordinates analysis (PCoA) depicting the community composition of the bacterial and archaeal communities based on the 16S rRNA gene. Colors refer to hydrologic treatments: brown indicates dry, light blue indicates interim, and dark blue indicates wet. Shapes refer to the hydrologic history of the sample: a square indicates dry, a triangle indicates interim, and a circle indicates wet. Open shapes refer to samples from mesocosms without plants, while closed shapes refer to samples from mesocosms with plants. Labeled vectors represent relationships among soil physicochemical variables and the microbial community ordination, with $p \leq 0.05$, scaled by their correlation (using the *envfit* function). Abbreviations: CEC: cation exchange capacity.

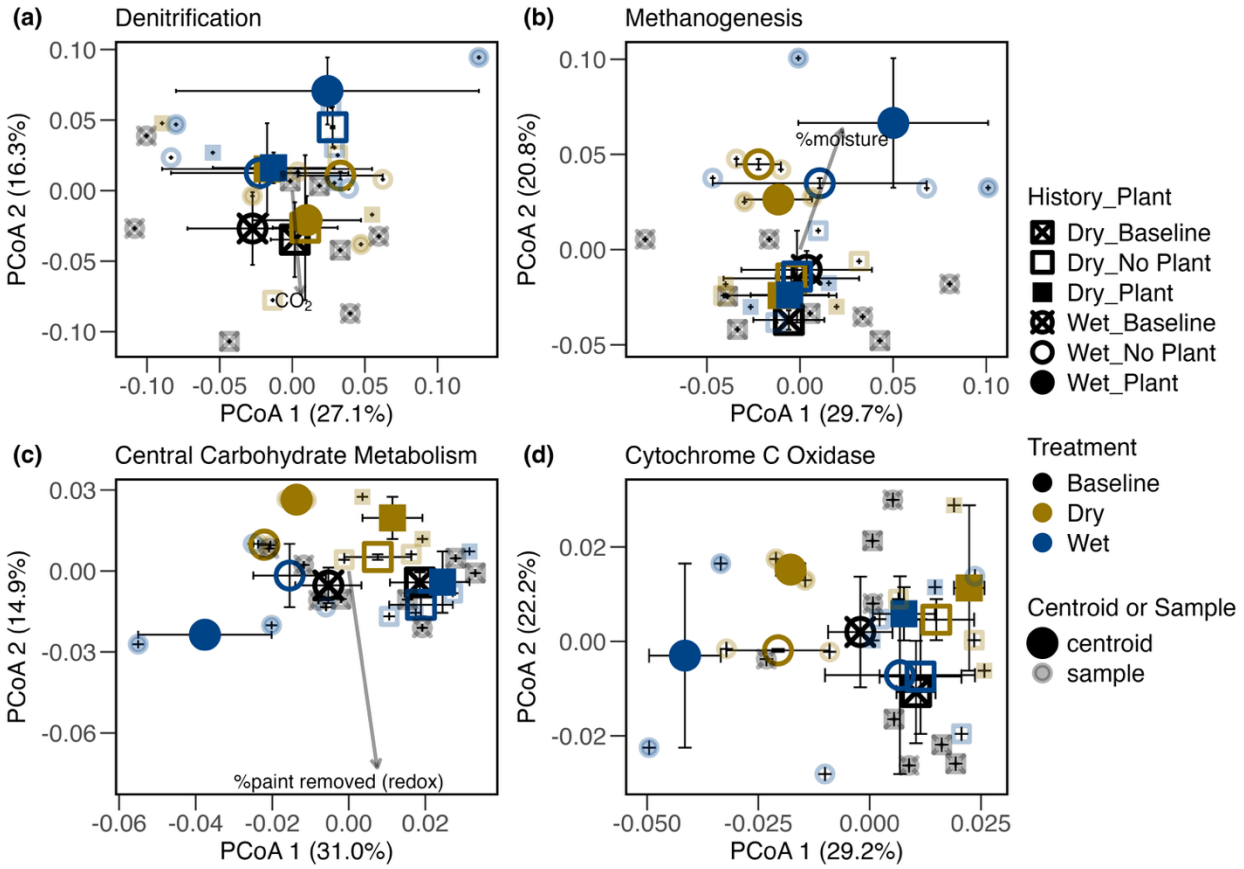

Figure 6. Ordination based on a principal coordinates analysis (PCoA) depicting community composition of the functional gene modules. The PCoA ordination is based on the Bray-Curtis distance of relative abundance of functional genes within respective KEGG modules: Panel (a): Denitrification (KEGG Module M00529), (b): Methanogen (M00617), (c): Central Carbohydrate Metabolism (M00001-M00011, M00307-M00309, M00580, and M00633), (d): Prokaryotic Cytochrome C Oxidase (M00155). Colors refer to hydrologic treatments: black represents the baseline, brown represents dry conditions, and dark blue represents wet conditions. Shapes refer to the hydrologic history of the sample: a square indicates dry, a triangle indicates interim, and a circle indicates wet. The shape fill represents plant treatment: cross = baseline, open = no plant, closed = plant. Baseline samples were collected prior to the initiation of hydrologic and plant treatments. Large, dark, opaque points represent centroids of samples within a group, while

smaller transparent points represent individual samples. Vectors represent significant ($p \leq 0.1$) relationships among greenhouse gas fluxes, soil physicochemical factors, and functional gene composition, with the length of the vectors scaled by the strength of correlation (using the *envfit* function).